

FORMFACTORS FOR INELASTIC SCATTERING BETWEEN HEAVY IONS

R.A. BROGLIA, C.H. DASSO, G. POLLAROLO and A. WINTHER

*The Niels Bohr Institute, University of Copenhagen,
Copenhagen, Denmark*



NORTH-HOLLAND PUBLISHING COMPANY – AMSTERDAM

FORMFACTORS FOR INELASTIC SCATTERING BETWEEN HEAVY IONS

R.A. BROGLIA*, C.H. DASSO, G. POLLAROLO** and A. WINTHER

The Niels Bohr Institute, University of Copenhagen, Copenhagen, Denmark

Received May 1978

Abstract:

The formfactors associated with inelastic scattering of heavy ions are calculated in terms of single-particle wavefunctions and the corresponding shell model potential. The formalism parallels the one utilized in the description of one- and two-particle transfer reactions, and can be incorporated in a nuclear field theory. The macroscopic formfactors for vibrational states commonly used in the analysis of experiments are shown to be more accurate than hitherto assumed.

Contents:

1. Introduction	353	Appendix A: Microscopic formfactors for superfluid and deformed nuclei	374
2. Microscopic calculation of the formfactors	353	Appendix B: Matrix elements between multi-phonon states	377
3. Phonon excitation	359	Appendix C: Macroscopic formfactor for deformed nuclei	378
4. Macroscopic formfactors	367	References	382
5. Equivalence of macroscopic and microscopic formfactors for collective states	371		
6. Differential cross-sections	373		
7. Conclusions	373		

Single orders for this issue

PHYSICS REPORTS (Review Section of Physics Letters) 48, No. 5 (1978) 351–382.

Copies of this issue may be obtained at the price given below. All orders should be sent directly to the Publisher. Orders must be accompanied by check.

Single issue price Dfl. 16.00, postage included.

*Also State University of New York, Department of Physics, Stony Brook, New York 11794, U.S.A.

**On leave from Istituto di Fisica Teorica dell'Universita degli Studi, and I.N.F.N. Sezione di Torino, Italy.

1. Introduction

A basic quantity describing grazing collisions between heavy ions is the ion–ion potential. From systematic analysis of elastic scattering data with the optical model one has determined the tail of this potential. It seems to compare well with the potential obtained by folding the densities of the two colliding nuclei with an effective nucleon-nucleon force (cf. e.g. [1]). The absorptive potential, which is utilized to account for the depopulation of the entrance channel shows, on the other hand, large variations from case to case.

Allowing the radii of the two ions to depend on the angles it is possible to obtain a description of inelastic processes (cf. e.g. [2]). The associated complex formfactors are proportional, for the case of monopole–multipole excitations, to the static or dynamic deformation of the nuclear systems, the radial dependence being given by the derivative of the optical potential. This macroscopic model of inelastic processes, which has been very successful in the analysis of experimental data, implies a proportionality between the variation of the density and the variation of the nuclear potential (cf. ref. [3]).

A rather detailed microscopic description of the different collective modes of excitation of the nucleus exists, in particular of rotations and vibrations. In the present paper, the corresponding formfactors are calculated in a representation which makes explicit reference to the individual neutrons and protons. The collective nature of the states excited in the scattering process is contained in the configuration mixing of the corresponding wavefunctions.

The inelastic scattering formfactors are thus calculated on the same footing as the one- and two-particle transfer formfactors (cf. e.g. [4]). A question of special interest to be investigated is the role played by the “hot orbitals”, i.e., orbitals which are particularly suited to respond to the external probe in an inelastic process.

In section 2 we derive the general expression for the microscopic formfactors following closely the notation utilized in ref. [4]. They are evaluated within the framework of nuclear structure models in section 3 and appendix A. The resulting quantities can be directly used in first order perturbation theory, or in a coupled channel calculation involving inelastic processes. The macroscopic formfactors corresponding to surface vibrations are derived in section 4, while the macroscopic formfactors for deformed nuclei are dealt with in appendix C. A discussion of the theoretical aspects of the comparison of these formfactors with the corresponding microscopic formfactors is presented in section 5. In section 6 we show some examples where microscopic and macroscopic formfactors are used to calculate differential cross-sections.

2. Microscopic calculation of the formfactors

We consider the process

$$b + B \rightarrow b' + B', \quad (2.1)$$

where b and B are two interacting ions. The primes on b and B indicate that the corresponding nuclei are in excited states.

The basic quantity to be calculated is the amplitude

$$\begin{aligned}
\langle\langle I'_\beta I'_\beta \rangle SN | f | (I_\beta I_\beta) SN \rangle_{r_{bB}} &= \sum_{\substack{m'_\beta m'_\beta, M'_b M'_b \\ M_B M_B}} \langle I'_\beta m'_\beta I'_\beta M'_\beta | SN \rangle \langle I_\beta m_\beta I_\beta M_\beta | SN \rangle \langle I'_b M'_b I'_B M'_B | I'_\beta M'_\beta \rangle \langle I_b M_b I_B M_B | I_\beta M_\beta \rangle \\
&\times \int r_{bB}^2 d\Omega_{r_{bB}} Y_{I'_\beta m'_\beta}^*(\hat{r}_{bB}) Y_{I_\beta m_\beta}(\hat{r}_{bB}) \int d\xi_b d\xi_B \psi_{I'_b M'_b}^{b*}(\xi_b) \psi_{I'_B M'_B}^{B*}(\xi_B) \\
&\times (V_{bB} - U_{bB}) \psi_{I_b M_b}^b(\xi_b) \psi_{I_B M_B}^B(\xi_B),
\end{aligned} \quad (2.2)$$

where the wavefunctions $\psi_{I_b M_b}^b$ and $\psi_{I_B M_B}^B$ describe the states of the nucleus b and B , respectively, ξ_b and ξ_B being the corresponding intrinsic coordinates.

The angular momentum of relative motion in channel $(b + B) \equiv \beta$ is denoted by I_β and it is coupled to the total intrinsic angular momentum I_β of the nuclei b and B . The resulting channel spin S is a conserved quantity. The corresponding quantities associated with the channel $(b' + B') \equiv \beta'$ are indicated by the same symbols, but primed. The potential V_{bB} is the interaction between all the nucleons in b with all the nucleons in B , while U_{bB} is the expectation value of this quantity. Note that the coordinate of relative motion of both channels coincide. We shall thus in the following drop the label on this variable.

The integral in (2.2), usually referred to as the formfactor, can be expanded in tensor components, i.e.,

$$\begin{aligned}
f_{\beta\beta'}(\mathbf{r}) &= \int d\xi_b d\xi_B \psi_{I'_b M'_b}^{b*}(\xi_b) \psi_{I'_B M'_B}^{B*}(\xi_B) (V_{bB} - U_{bB}) \psi_{I_b M_b}^b(\xi_b) \psi_{I_B M_B}^B(\xi_B) \\
&= \sum_{\substack{JJ'\lambda \\ MM'\mu}} \langle I_B M_B J M | I'_B M'_B \rangle \langle I'_b M'_b J' M' | I_b M_b \rangle \langle \lambda \mu J M | J' M' \rangle f_{\lambda\mu}^{JJ'}(\mathbf{r}),
\end{aligned} \quad (2.3)$$

or equivalently

$$f_{\lambda\mu}^{JJ'}(\mathbf{r}) = \frac{(2J+1)(2\lambda+1)}{(2I'_B+1)(2I_b+1)} \sum_{\substack{M_b M_B \\ M'_b M'_B}} \langle I_B M_B J M | I'_B M'_B \rangle \langle I'_b M'_b J' M' | I_b M_b \rangle \langle \lambda \mu J M | J' M' \rangle f_{\beta\beta'}(\mathbf{r}), \quad (2.4)$$

J and J' being the angular momenta transferred between the target and the residual nucleus and between the projectile and the outgoing particle respectively, while λ is the angular momentum transferred between the orbital and the intrinsic motion. Since the function $f_{\lambda\mu}^{JJ'}(\mathbf{r})$ is a tensor of rank λ , one can obtain the explicit dependence on two of its variables, utilizing an intrinsic system whose z -axis is along the relative position vector \mathbf{r} , i.e.

$$f_{\lambda\mu}^{JJ'}(\mathbf{r}) = \sum_{\mu'} \mathcal{D}_{\mu\mu'}^\lambda(\varphi, \theta, 0) [f_{\lambda\mu'}^{JJ'}(\mathbf{r})]_{\text{intr.}} \quad (2.5)$$

The formfactor $[f_{\lambda\mu'}^{JJ'}(\mathbf{r})]_{\text{intr.}}$ is given by the same expression (2.4) except that it is evaluated in a coordinate system where \mathbf{r} is the quantization axis. Because of the axial symmetry around this vector, only the term with $\mu' = 0$ in (2.5) contributes and we thus define the radial formfactor by the equation

$$f_{\lambda\mu}^{JJ'}(\mathbf{r}) = f_\lambda^{JJ'}(\mathbf{r}) Y_{\lambda\mu}(\hat{\mathbf{r}}), \quad (2.6)$$

where

$$f_{\lambda}^{JJ'}(r) = \sqrt{\frac{4\pi}{2\lambda + 1}} [f_{\lambda 0}^{JJ'}(r)]_{\text{intr.}} \quad (2.7)$$

Performing a reflection in a plane containing the r -axis it is seen that the formfactor (2.7) vanishes unless

$$\lambda + \pi = \text{even} \quad (2.8)$$

where π is the parity change taking place in the reaction. This selection rule is valid insofar as one can neglect velocity dependent interactions, in particular the interactions inducing magnetic excitations (cf. ref. [5] section IV.5).

In order to express the formfactor (2.7) in terms of the single-particle degrees of freedom we use the fractional parentage expansions

$$\psi_{I_B M_B}^B(\xi_C, r_{1C}, \xi_1) = \sum_{Cjm} \langle I_C M_C j m | I_B M_B \rangle \varphi_{jm}^{B(C)}(r_{1C}, \xi_1) \psi_{I_C M_C}^C(\xi_C), \quad (2.9)$$

and

$$\psi_{I_b M_b}^b(\xi_c, r_{2c}, \xi_2) = \sum_{c'j'm'} \langle I_c M_c j' m' | I_b M_b \rangle \varphi_{j'm'}^{b(c)}(r_{2c}, \xi_2) \psi_{I_c M_c}^c(\xi_c), \quad (2.10)$$

and correspondingly for the excited states. Inserting these expansions in (2.3) we find

$$f_{\beta\beta'}(\mathbf{r}) = [f_{\beta\beta'}(\mathbf{r})]_{\text{target}} + [f_{\beta\beta'}(\mathbf{r})]_{\text{projectile}} + [f_{\beta\beta'}(\mathbf{r})]_{\text{mutual}} + [f_{\beta\beta'}(\mathbf{r})]_{\text{recoil}}, \quad (2.11)$$

where

$$\begin{aligned} [f_{\beta\beta'}(\mathbf{r})]_{\text{target}} &= \delta(b, b') \sum_{C, m_1, m_2} \langle I_C M_C j_1 m_1 | I_B M_B \rangle \langle I_C M_C j_2 m_2 | I'_B M'_B \rangle \int \varphi_{j_2 m_2}^{B(C)*}(r_{1C}, \xi_1) U_{1b}(r_{1b}) \\ &\quad \times \varphi_{j_1 m_1}^{B(C)}(r_{1C}, \xi_1) d^3 r_1 d\xi_1, \end{aligned} \quad (2.12)$$

gives rise to target excitation while

$$\begin{aligned} [f_{\beta\beta'}(\mathbf{r})]_{\text{projectile}} &= \delta(B, B') \sum_{c, m'_1, m'_2} \langle I_c M_c j'_1 m'_1 | I_b M_b \rangle \langle I_c M_c j'_2 m'_2 | I'_b M'_b \rangle \int \varphi_{j'_2 m'_2}^{b(c)*}(r_{1c}, \xi_1) U_{1B}(r_{1B}) \\ &\quad \times \varphi_{j'_1 m'_1}^{b(c)}(r_{1c}, \xi_1) d^3 r_1 d\xi_1, \end{aligned} \quad (2.13)$$

induces projectile excitation.

In the above expressions U_{ij} indicates the expectation value of the interaction V_{ij} over all coordinates not specified. The quantity $U_{1b}(r_{1b})$ is thus the expectation value of the interaction $V_{1b}(\xi_c, r_{2c}, r_{1b})$ over the degrees of freedom of c and of particle 2, i.e., it is the shell model potential for the particle 1 moving in b . We have assumed that these expectation values do not depend on the magnetic quantum numbers.

The third term in (2.11) indicates mutual excitation, being non-diagonal in both target and projectile quantum numbers. The main term here is the matrix element of $V_{12}(r_{12})$.

The fourth term is given by

$$\begin{aligned}
& [f_{\beta\beta'}(\mathbf{r})]_{\text{recoil}} \\
&= \sum_{\substack{cCm_1m'_1 \\ m_2m'_2}} \langle I_C M_C j_1 m_1 | I_B M_B \rangle \langle I_C M_C j_2 m_2 | I'_B M'_B \rangle \langle I_c M_c j'_1 m'_1 | I_b M_b \rangle \langle I_c M_c j'_2 m'_2 | I'_b M'_b \rangle \int d^3r_1 d^3r_2 d\xi_1 d\xi_2 \\
&\quad \times \varphi_{j_2 m_2}^{B(C)*}(\mathbf{r}_{1C}, \xi_1) \varphi_{j'_2 m'_2}^{b(c)*}(\mathbf{r}_{2c}, \xi_2) \left\{ U_{cC} \left(\mathbf{r} + \frac{m_1}{m_B} \mathbf{r}_{1C} - \frac{m_2}{m_b} \mathbf{r}_{2c} \right) + \delta(b, b') U_{2C} \left(\mathbf{r} + \frac{m_1}{m_B} \mathbf{r}_{1C} \right) \right. \\
&\quad \left. + \delta(B, B') U_{1c} \left(\mathbf{r} - \frac{m_2}{m_b} \mathbf{r}_{2c} \right) + \delta(b, b') \delta(B, B') [U_{12}(\mathbf{r}) - U_{bB}(\mathbf{r})] \right\} \varphi_{j_1 m_1}^{B(C)}(\mathbf{r}_{1C}, \xi_1) \varphi_{j'_1 m'_1}^{b(c)}(\mathbf{r}_{2c}, \xi_2).
\end{aligned} \tag{2.14}$$

The different non-diagonal contributions arise as recoil effects due to the fact that $\mathbf{r} = \mathbf{r}_{bB}$ is kept fixed in evaluating the formfactor. For instance, the first and second terms in (2.14) induce target excitations. They can be included in (2.12) by substituting $U_{ib}(\mathbf{r}_{ib})$ by

$$U_{ib}(\mathbf{r}_{ib}) + U_{bC} \left(\left| \mathbf{r} + \frac{m_1}{m_B} \mathbf{r}_{1C} \right| \right) \approx U_{ib}(\mathbf{r}_{ib}) + \frac{m_1}{m_B} \mathbf{r}_{1C} \cdot \nabla U_{bC}(\mathbf{r}), \tag{2.15}$$

where m_B and m_1 are the masses of B and particle 1 respectively. Thus, the recoil term to lowest order contributes only to dipole excitation.

In deriving (2.11) we have neglected terms nondiagonal in the cores c and C. These terms are diagonal in the particle states i.e., the terms non-diagonal in c are diagonal in the state of particle 2 (but not necessarily in particle 1). If the non-diagonal terms in c and C are important one should exhibit more particle degrees of freedom until the remaining core is inert, and the total formfactor would be the sum of formfactors of the type (2.11)–(2.15) over all valence particles.

In the following we neglect the mutual excitation as well as the recoil term (2.14). For target excitation we thus have

$$\begin{aligned}
f_{\beta\beta'}(\mathbf{r}) &= \sum_{c j_1 m_1 j_2 m_2} C^*(I_C a_2; I'_B) C(I_C a_1; I_B) \langle I_C M_C j_1 m_1 | I_B M_B \rangle \langle I_C M_C j_2 m_2 | I'_B M'_B \rangle \\
&\quad \times \int d^3r_1 d\xi_1 \phi_{j_2 m_2}^{(C)*}(a_2, \mathbf{r}_{1C}, \xi_1) U_{ib}(\mathbf{r}_{ib}) \phi_{j_1 m_1}^{(C)}(a_1, \mathbf{r}_{1C}, \xi_1),
\end{aligned} \tag{2.16}$$

where according to the notation utilized[†] in ref. [4]

$$\varphi_{j_2 m_2}^{B(C)}(\mathbf{r}_{1C}, \xi_1) = C(I_C a_2; I'_B) \phi_{j_2 m_2}^{(C)}(a_2; \mathbf{r}_{1C}, \xi_1) \tag{2.17}$$

and

$$\varphi_{j_1 m_1}^{B(C)}(\mathbf{r}_{1C}, \xi_1) = C(I_C a_1; I_B) \phi_{j_1 m_1}^{(C)}(a_1; \mathbf{r}_{1C}, \xi_1). \tag{2.18}$$

The quantity C is the single-particle spectroscopic amplitude defined as

$$C(I_C a_1; I_B) \equiv \langle I_B \| a_{j_1}^+(a_1) \| I_C \rangle^* / \sqrt{2I_B + 1}. \tag{2.19}$$

[†] A consistency between the phase conventions used in ref. [4] for states defined in second quantization or in configuration space is achieved only by giving the radial wave function $R_j(r)$ a phase i^l , and table 3 and 4 of that reference should be changed accordingly. In the present paper we consistently use the so-called Condon and Shortley convention.

Here $a_{j_1 m_1}^+(a_1)$ creates a particle in the state a_1 , m_1 , where a_1 stands for the radial, orbital and total angular momentum quantum numbers n_1 , l_1 and j_1 respectively. The associated wavefunction in configuration space is

$$\phi_{j_1 m_1}^{(C)}(a_1; r_{1C}; \xi_1) = R_{a_1}^{(C)}(r_{1C}) [Y_{l_1}(\hat{r}_{1C}) \chi(\xi_1)]_{j_1 m_1}, \quad (2.20)$$

where the square bracket indicates vector coupling. The function $R_{a_1}^{(C)}(r_{1C})$ is the normalized radial wavefunction while $\chi(\xi_1)$ is the spin function.

We can rewrite (2.16) in the form

$$f_{\beta\beta'}(\mathbf{r}) = \sum_{C j_1 m_1 j_2 m_2 \lambda \mu} C^*(I_C a_2; I'_B) C(I_C a_1; I_B) \langle I_C M_C j_1 m_1 | I_B M_B \rangle \langle I_C M_C j_2 m_2 | I'_B M'_B \rangle \langle j_1 m_1 \lambda - \mu | j_2 m_2 \rangle \\ \times \frac{(-1)^{\lambda + \mu}}{\sqrt{2\lambda + 1}} f_{\lambda\mu}^{(a_1 a_2) \lambda 0}(\mathbf{r}), \quad (2.21)$$

where the single-particle formfactor is defined by

$$f_{\lambda\mu}^{a_2 a_1}(\mathbf{r}) = \frac{(2\lambda + 1)^{\frac{1}{2}}}{2j_2 + 1} (-1)^{\lambda - \mu} \sum_{m_1 m_2} \langle j_1 m_1 \lambda - \mu | j_2 m_2 \rangle \int d^3 r_1 d\xi_1 \phi_{j_2 m_2}^{(a_2)*}(a_2; r_{1C} \xi_1) U_{1b}(r_{1b}) \\ \times \phi_{j_1 m_1}^{(a_1)}(a_1; r_{1C} \xi_1). \quad (2.22)$$

Formulating this result in second quantization we generalize $f_{\beta\beta'}$ to include the excitation of correlated states. We thus define an operator $\hat{f}(\mathbf{r})$ such that its matrix elements are equal to (2.16), i.e.

$$\hat{f}(\mathbf{r}) = \sum_{\substack{a_1 a_2 \\ \lambda \mu}} (-1)^{\lambda + \mu + \pi_1} \frac{\sqrt{2j_2 + 1}}{2\lambda + 1} f_{\lambda\mu}^{a_2 a_1}(\mathbf{r}) [a_{j_2}^+(a_2) b_{j_1}^+(a_1)]_{(j_2 j_1) \lambda, -\mu}, \quad (2.23)$$

where $b_{j_1 m_1}^+(a_1) = (-1)^{j_1 + m_1 + \pi_1} a_{j_1 - m_1}$ creates a hole in the orbital a_1 and where

$$[a_{j_2}^+(a_2) b_{j_1}^+(a_1)]_{\lambda\mu} = \sum_{m_1 m_2} \langle j_2 m_2 j_1 m_1 | \lambda \mu \rangle a_{j_2 m_2}^+(a_2) b_{j_1 m_1}^+(a_1) = (-1)^{j_1 - j_2 + \lambda + \mu} [a_{j_1}^+(a_1) b_{j_2}^+(a_2)]_{\lambda - \mu}^+. \quad (2.24)$$

The quantity π_1 is the parity of the single particle state. One may easily verify the identity

$$\langle I'_B M'_B | \hat{f} | I_B M_B \rangle = f_{\beta\beta'}(\mathbf{r}). \quad (2.25)$$

The expression (2.22) for the single particle formfactor appearing in (2.23) can be reduced making use of the single-particle wavefunction (2.20) and of the relation

$$\begin{pmatrix} l_1 & l_2 & \lambda \\ 0 & 0 & 0 \end{pmatrix} \begin{pmatrix} j_2 & j_1 & \lambda \\ l_1 & l_2 & \frac{1}{2} \end{pmatrix} = - \frac{(-1)^{j_2 - j_1}}{\sqrt{(2l_1 + 1)(2l_2 + 1)(2\lambda + 1)}} \langle j_2 \frac{1}{2} j_1 - \frac{1}{2} | \lambda 0 \rangle \delta(l_1 + l_2 + \lambda, \text{even}). \quad (2.26)$$

One thus finds

$$f_{\lambda\mu}^{a_2 a_1}(\mathbf{r}) = f_{\lambda}^{a_2 a_1}(\mathbf{r}) Y_{\lambda\mu}(\hat{\mathbf{r}}),$$

with

$$f_{\lambda}^{a_2 a_1}(r) = \sqrt{\pi} \sqrt{(2\lambda + 1)(2j_1 + 1)} (-1)^{j_2 - 1/2} \langle j_2 \frac{1}{2} j_1 - \frac{1}{2} | \lambda 0 \rangle \delta(l_1 + l_2 + \lambda, \text{even}) \int_0^{\infty} r_{1c}^2 dr_{1c} \\ \times \int_{-1}^1 d(\cos \theta) R_{a_2}^{(\odot)*}(r_{1c}) U_{1b}(\sqrt{r_{1c}^2 + r^2 - 2rr_{1c} \cos \theta}) R_{a_1}^{(\odot)}(r_{1c}) P_{\lambda}(\cos \theta). \quad (2.27)$$

Since we work with real radial wavefunctions the formfactor (2.27) is real and satisfies the general symmetry property

$$f_{\lambda}^{a_1 a_2}(r) = (-1)^{j_1 - j_2} \sqrt{\frac{2j_2 + 1}{2j_1 + 1}} f_{\lambda}^{a_2 a_1}(r). \quad (2.28)$$

An alternative way of writing the formfactor (2.23) is

$$f(r) = \int U_{1b}(r'_{1b}) \hat{\rho}(r'_{1c}) d^3 r_1, \quad (2.29)$$

where the density operator $\hat{\rho}$ is defined by

$$\hat{\rho}(r_{1c}) = \sum_{\substack{a_1 a_2 \\ m_1 m_2}} \int d\xi_1 \phi_{j_2 m_2}^*(a_2; r_{1c} \xi_1) \phi_{j_1 m_1}(a_1; r_{1c} \xi_1) a_{j_2 m_2}^+(a_2) a_{j_1 m_1}(a_1). \quad (2.30)$$

It should be noted that the diagonal matrix elements of (2.23) and (2.29) are nonvanishing, in contrast to the diagonal part of (2.3) which is zero. The diagonal part of (2.29) is the ion-ion potential as obtained by folding.

As an example of the formalism derived above we consider first formfactors for two particles outside closed shell. We assume that the core of the nucleus remains inert during the process of excitation. The generalization to the case where ground state correlations are included is discussed below. The ground state is described by the wavefunction

$$|I_B M_B\rangle \equiv |00\rangle = \sum_{a_1} X(a_1 a_1; I_B = 0) \frac{[a_{j_1}^+(a_1) a_{j_1}^+(a_1)]_{00}}{\sqrt{2}} |0\rangle, \quad (2.31)$$

where X is the amplitude of the different two-particle configurations and the square brackets indicate the vector coupling of the two angular momenta to $I_B = M_B = 0$. The state $|0\rangle$ indicates the closed shell system, which is also the vacuum of the operators a_{jm}^+ . The wavefunction of the excited state is given by

$$|I_B' M_B'\rangle \equiv |\lambda\mu\rangle = \sum_{a_1 \geq a_2} X(a_1 a_2; I_B = \lambda) \frac{[a_{j_1}^+(a_1) a_{j_2}^+(a_2)]_{\lambda\mu}}{\sqrt{1 + \delta(a_1, a_2)}} |0\rangle. \quad (2.32)$$

The matrix element of the operator (2.23) between the two states defined above can be written as

$$\langle \lambda\mu | f | 00 \rangle = f_{\beta\beta'}(r) \\ = \sqrt{2} \sum_{a_2 \geq a_1} \frac{\sqrt{2j_1 + 1}}{2\lambda + 1} \frac{X(a_1 a_2; \lambda)}{\sqrt{1 + \delta(a_1, a_2)}} \left[\frac{X(a_1 a_1; 0)}{\sqrt{2j_1 + 1}} + (-1)^{\lambda} \frac{X(a_2 a_2; 0)}{\sqrt{2j_2 + 1}} \right] f_{\lambda\mu}^{a_1 a_2}(r). \quad (2.33)$$

3. Phonon excitation

The inelastic formfactors were derived in the previous section in terms of wavefunctions expressed in a fermion basis. It has proved useful to describe the nucleus in terms of elementary modes of excitation where both fermion and boson degrees of freedom are utilized [3]. The two types of bosons entering in this picture are those corresponding to correlated particle-hole states (wavy line in fig. 1) and correlated two particle states (double arrowed line in fig. 1). The field generated by the projectile can, in this picture, either change the state of motion of a particle as for instance in graphs (a) and (f) of fig. 1 or it can create a particle-hole boson, as in graphs (b) and (d).

The formfactor (2.33) calculated in the previous section corresponds to the evaluation of graph (a). The quantity $X(a_1 a_1; 0)$ is the amplitude for the ground state boson on the configuration (a_1, a_1) while $X(a_1 a_2; \lambda)$ is the amplitude describing the configuration (a_1, a_2) in the excited state λ (cf. eqs. (2.32) and (2.31)).

In order to evaluate graph (b) we should recast the operator (2.23) in terms of the boson operators. In the random phase approximation (RPA) the boson operator is defined as

$$\Gamma_{\lambda\mu}^+(n) = \sum_{a_i a_k} \{X(a_k a_i; \lambda) \Gamma_{\lambda\mu}^+(a_k a_i) + (-1)^\mu Y_n(a_k a_i; \lambda) \Gamma_{\lambda-\mu}(a_k a_i)\}, \quad (3.1)$$

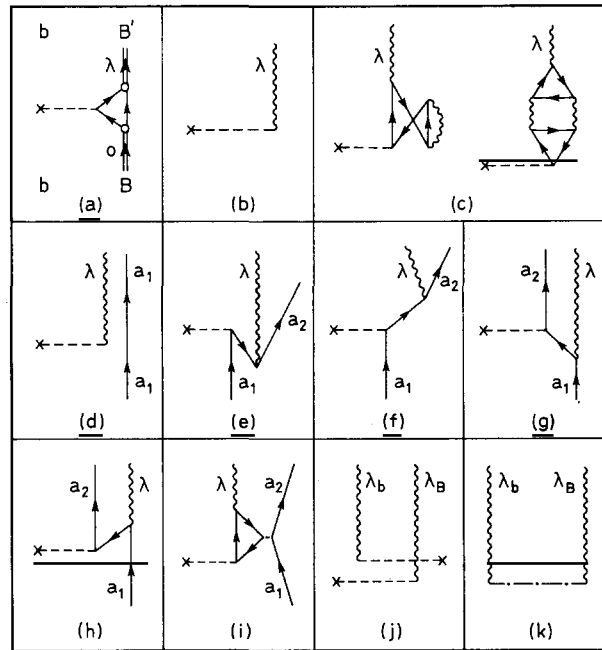


Fig. 1. Graphical representation of inelastic scattering. The graphs (a)–(i) represent the excitation of the target nucleus through the field of the projectile, while (j) and (k) represent excitation of both systems. The excitation of the pairing vibration in (a) takes place through a particle excitation, after the phonon has been decomposed into a two-particle state. The graph (b) indicates the excitation of a surface vibrational phonon in a closed systems. Two of the graphs representing the higher order corrections to this process are depicted in (c).

The graphs (d)–(i) indicate the excitation of a surface vibrational mode in an odd system. The lowest order graph in (d) is dominant, if the phonon is strongly collective.

The graph (j) indicates the second order process in which the phonon is excited in both target and projectile (simultaneous excitations), while graph (k) is the mutual excitation of two phonons taking place through the interaction $f_{\beta\beta'}(r)_{\text{mutual}}$ in (2.11).

acting on the correlated ground state $|\tilde{0}\rangle$ defined by the relation

$$\Gamma_{\lambda\mu}(n)|\tilde{0}\rangle = 0. \quad (3.2)$$

In the following we use the convention as in (3.1) that the index k is used for particle states and the index i for hole states. The quantities X and Y are the forward-going and backward-going amplitudes and are obtained by diagonalizing the residual Hamiltonian in RPA. The index n indicates the corresponding eigenvalue. The operator $\Gamma_{\lambda\mu}^+(a_1, a_2)$ is defined as

$$\Gamma_{\lambda\mu}^+(a_k a_i) = [a_{jk}^+ (a_k) b_{ji}^+ (a_i)]_{\lambda\mu}. \quad (3.3)$$

From the commutation relations

$$[\Gamma_{\lambda\mu}(n), \Gamma_{\lambda\mu}^+(m)] = \delta(n, m), \quad (3.4)$$

and

$$[\Gamma_{\lambda\mu}(n), \Gamma_{\lambda\mu}(n)] = [\Gamma_{\lambda\mu}^+(n), \Gamma_{\lambda\mu}^+(m)] = 0, \quad (3.5)$$

we can express the particle-hole operator (3.3) in terms of the collective operators $\Gamma_{\lambda\mu}^+(n)$ and $\Gamma_{\lambda\mu}(n)$. One thus obtains:

$$\Gamma_{\lambda\mu}^+(a_k a_i) = \sum_n [X_n(a_k a_i; \lambda) \Gamma_{\lambda\mu}^+(n) - (-1)^\mu Y_n(a_k a_i; \lambda) \Gamma_{\lambda-\mu}(n)]. \quad (3.6)$$

Observing that the formfactor (2.23) can be rewritten as

$$\begin{aligned} \hat{f}(r) = & \sum_{\substack{a_1 \geq a_2 \\ \lambda\mu}} \frac{1}{(2\lambda+1)(1+\delta(a_1, a_2))} (-1)^{\lambda+\mu} \{(-1)^{\pi_1} (2j_2+1)^{1/2} f_{\lambda\mu}^{a_2 a_1}(r) [a_{j_2}^+(a_2) b_{j_1}^+(a_1)]_{\lambda-\mu} \\ & + (-1)^{\pi_2} (2j_1+1)^{1/2} f_{\lambda\mu}^{a_1 a_2}(r) [a_{j_1}^+(a_1) b_{j_2}^+(a_2)]_{\lambda-\mu}\}, \end{aligned}$$

and utilizing the relations (2.24) and (2.28) we obtain the following expression for the formfactor in terms of the boson operator (3.1)

$$(\hat{f}(r))_B = \sum_n \frac{1}{\sqrt{2\lambda+1}} (-1)^{\lambda+\mu} f_{\lambda-\mu}^n(r) [\Gamma_{\lambda\mu}^+(n) + (-1)^\mu \Gamma_{\lambda-\mu}(n)], \quad (3.7)$$

where

$$f_{\lambda\mu}^n(r) = \sum_{a_i a_k} \sqrt{\frac{2j_k+1}{2\lambda+1}} (-1)^{\pi_i} f_{\lambda\mu}^{a_k a_i}(r) [X_n(a_k a_i; \lambda) - Y_n(a_k a_i; \lambda)]. \quad (3.8)$$

To lowest order the graph 1(b) or the corresponding matrix element of (3.7), $\langle \lambda\mu | \hat{f} | \tilde{0} \rangle$, describes the excitation of vibrational quanta. In a closed shell system the corrections to this description arise from graphs of type (c) in fig. 1. For an odd system the corresponding corrections are given by graphs (e)–(i), the lowest order graph being given by (d).

To calculate systematically the formfactors within the framework of the nuclear field theory [6] one thus has to utilize both the boson representation (3.7) of the formfactor and the fermion representation

$$(\hat{f}(r))_F = \sum_{\substack{a_1 a_2 \\ \lambda\mu}} (-1)^{\lambda+\mu+\pi_1} \frac{\sqrt{2j_2+1}}{2\lambda+1} f_{\lambda-\mu}^{a_2 a_1}(r) [a_{j_2}^+(a_2) b_{j_1}^+(a_1)]_{\lambda\mu}. \quad (3.9)$$

The generalization of (3.7) and (3.9) to the case of pairing deformed (superfluid) and shape deformed nuclei is worked out in the appendix A.

Note that all formfactors include components responsible for Coulomb excitation. Thus for values of r larger than the sum of the radii R_b and R_B of the two nuclei b and B we may expand the Coulomb part of the single-particle potential in (2.22) as

$$U_{1b}(|r_{1C} - r|) = Z_b e \sum_{\lambda\mu} \frac{4\pi e_1}{2\lambda + 1} Y_{\lambda\mu}^*(\hat{r}_{1C}) Y_{\lambda\mu}(\hat{r}) r_{1C}^\lambda r^{-\lambda-1}, \quad (3.10)$$

Z_b being the charge number of the projectile. This leads to

$$f_{\lambda\mu}^{a_2 a_1}(r) = \frac{4\pi Z_b e}{\sqrt{(2\lambda + 1)(2j_2 + 1)}} (-1)^\lambda \langle j_2 \| \mathcal{M}(E\lambda) \| j_1 \rangle r^{-\lambda-1} Y_{\lambda\mu}(\hat{r}), \quad (3.11)$$

where

$$\mathcal{M}(E\lambda\mu) = e_1 r_{1C}^\lambda Y_{\lambda\mu}(\hat{r}_1). \quad (3.12)$$

Inserting (3.11) in (3.8) we find for the Coulomb excitation of a phonon

$$f_{\lambda\mu}^n(r) = \frac{4\pi Z_b e}{2\lambda + 1} (-1)^\lambda \langle n\lambda \| \mathcal{M}(E\lambda) \| 0 \rangle r^{-\lambda-1} Y_{\lambda\mu}(\hat{r}), \quad (3.13)$$

where the collective reduced matrix element of the electric multipole operator is given by

$$\langle n\lambda \| \mathcal{M}(E\lambda) \| 0 \rangle = \sum_{a_1 a_2} (-1)^{\pi_2} [X_n(a_1 a_2; \lambda) - Y_n(a_1 a_2; \lambda)] \langle j_1 \| e_1 r_{1C}^\lambda Y_\lambda \| j_2 \rangle. \quad (3.14)$$

These quantities can be determined experimentally in a model independent way and thus provide a crucial test of the description of the nuclear states. A microscopic description which reproduces these numbers and at the same time reproduces the excitation energy is thus expected to lead also to a total formfactor (3.8) which is more accurate than the macroscopic formfactors which have mainly been used up to now.

The extent to which the micro- and macroscopic formfactors are the same will be studied in the following sections.

In the following we give examples of inelastic formfactors associated with both collective and non-collective vibrational states of ^{208}Pb and ^{120}Sn . Non-collective refers, in the present context, to states which are dominated by few components or states whose wavefunctions display destructive interference. Only quadrupole and octupole excitations are considered.

The calculations were carried out diagonalizing a schematic multipole–multipole force including both an isoscalar and an isovector term. The strength of the isoscalar force was chosen equal to the selfconsistent value (cf. [3], chapter 6)

$$\kappa(\lambda, \tau = 0) \approx \frac{4\pi}{3} \frac{41}{(1.2)^{2(\lambda-1)}} \frac{1}{A^{(\lambda+3)/3}} \left(\frac{M\omega_0}{\hbar} \right)^\lambda \text{ MeV}. \quad (3.15)$$

The ratio between the isoscalar and isovector strengths was set equal to (cf. refs. [3] and [7])

$$\kappa(\lambda, \tau = 1)/\kappa(\lambda, \tau = 0) \approx -0.45(3 + 2\lambda). \quad (3.16)$$

The particles were assumed to move in a harmonic oscillator potential and all $\Delta N = 0$ and 2 excitations were included in the case of the quadrupole mode, while all $\Delta N = 1$ and 3 excitations were included in the case of the octupole vibrations. The calculations for ^{120}Sn were based on equation (A.4) of appendix A. The quasiparticle occupation parameters, U , V were determined according to the standard BCS prescription. The spectra and wavefunctions for the collective 2^+ states of ^{208}Pb and ^{120}Sn are given in ref. [7]. The wavefunctions associated with the non-collective states utilized in the calculations of formfactors below are given in table 1. Using the same parameters, the 3^- states of ^{208}Pb were calculated. The properties of some of these states are given in table 3 and the corresponding wavefunctions are shown in table 4.

Table 1
Properties of the quadrupole non-collective states of ^{208}Pb and ^{120}Sn used in fig. 2. The energies E are given in column 2. For details on the contents of the other columns see the caption of table 3. The wavefunctions are given in table 2

	E	\mathcal{E}	\mathcal{N}	$\Lambda(1/2)/\sqrt{\kappa}$	$\Lambda(-1/2)/\sqrt{\kappa}$	R	RE
Pb(2^+)	12.73	2.66	0.56	0.61	-0.49	0.70	8.91
Sn(2^+)	4.65	1.7	0.09	0.73	-0.54	0.43	2.00

Table 2
Wavefunctions for two non-collective quadrupole modes of ^{120}Sn and ^{208}Pb , respectively, utilized in connection with fig. 2. Each configuration is characterized by the six quantum numbers $a_1 \equiv (N1, L1, J1)$ and $a_2 \equiv (N2, L2, J2)$. The quantity DN indicates the difference in the principal quantum number of the harmonic oscillator shells connected by the excitation. The forward-going and backward-going amplitudes are denoted by $X = X(a_1, a_2; \lambda)$ and $Y = Y(a_1, a_2; \lambda)$, respectively. For more details confer ref. [7], section 6. The quantity $2T = \pm 1$ labels neutron and proton excitations respectively

										$E = 12.73$					$E = 4.65$				
$N1$	$L1$	$J1$	$N2$	$L2$	$J2$	$2T$	DN	X	Y	$N1$	$L1$	$J1$	$N2$	$L2$	$J2$	$2T$	DN	X	Y
1.0	4.0	4.5	0.0	6.0	6.5	+1	0	0.03	0.01	1.0	2.0	1.5	1.0	2.0	1.5	+1	0	0.08	0.02
1.0	3.0	3.5	0.0	5.0	5.5	-1	0	0.02	0.01	0.0	4.0	3.5	0.0	4.0	4.5	-1	0	0.08	0.01
0.0	6.0	6.5	0.0	4.0	4.5	-1	2	0.07	0.01	1.0	2.0	1.5	0.0	4.0	3.5	+1	0	0.37	0.03
0.0	6.0	5.5	0.0	4.0	3.5	-1	2	0.14	0.01	2.0	0.0	0.5	1.0	2.0	2.5	+1	0	0.41	0.02
1.0	4.0	4.5	1.0	2.0	2.5	-1	2	0.13	0.01	0.0	4.0	3.5	1.0	2.0	2.5	+1	0	0.05	-0.00
0.0	7.0	7.5	0.0	5.0	5.5	+1	2	0.47	0.01	1.0	3.0	3.5	0.0	5.0	5.5	+1	0	0.08	-0.02
1.0	5.0	5.5	0.0	5.0	4.5	+1	2	0.04	0.00	1.0	2.0	1.5	2.0	0.0	0.5	+1	0	-0.10	-0.03
1.0	4.0	4.5	0.0	4.0	3.5	-1	2	0.04	0.00	0.0	5.0	5.5	0.0	5.0	5.5	+1	0	-0.18	-0.04
1.0	4.0	4.5	0.0	4.0	3.5	+1	2	0.09	-0.00	1.0	2.0	1.5	1.0	2.0	2.5	+1	0	-0.23	-0.01
1.0	4.0	4.5	1.0	2.0	2.5	+1	2	0.17	-0.01	1.0	2.0	1.5	0.0	4.0	4.5	-1	0	-0.73	-0.03
1.0	3.0	2.5	1.0	1.0	0.5	-1	2	0.06	-0.00	0.0	4.0	3.5	0.0	4.0	3.5	+1	0	-0.15	0.01
0.0	6.0	5.5	0.0	4.0	3.5	+1	2	0.16	-0.01	1.0	2.0	2.5	1.0	2.0	2.5	+1	0	-0.10	0.09
2.0	1.0	1.5	1.0	1.0	0.5	-1	2	0.02	-0.00	0.0	6.0	6.5	0.0	4.0	4.5	-1	2	-0.05	0.02
2.0	2.0	2.5	1.0	2.0	1.5	+1	2	0.02	-0.00	0.0	5.0	5.5	0.0	3.0	3.5	-1	2	0.03	-0.02
2.0	2.0	2.5	2.0	0.0	0.5	+1	2	0.04	-0.00	0.0	6.0	6.5	0.0	4.0	4.5	+1	2	0.05	-0.03
1.0	4.0	3.5	1.0	2.0	1.5	+1	2	0.06	-0.01	0.0	5.0	4.5	0.0	3.0	2.5	-1	2	0.03	-0.01
1.0	6.0	6.5	0.0	6.0	6.5	+1	2	0.02	-0.00	1.0	4.0	4.5	1.0	2.0	2.5	+1	2	0.03	-0.02

^{208}Pb (2^+) (non-collective)

^{120}Sn (2^+) (non-collective)

Table 3

Properties of octupole states in ^{208}Pb . In columns 1 and 2 the energies E and centroids E_c within the groups indicated are collected. The centroids are defined by $E_c = \sum_i R_i E_i / (\sum_i R_i)$ where R_i are the transition probabilities from the ground state given in column 7 (in single particle units). The multipole mass moments for protons (\mathcal{P}) and neutrons (\mathcal{N}) are displayed in column 3 and 4 in units of $(\hbar/M\omega_0) = A^{1/3} \text{ fm}^2$. In column 5 and 6 the neutron and proton particle-vibration coupling strengths as defined in ref. [7] are given. In column 7 the ratio $R = B(E3)/B_{\text{sp}}$ of the $B(E3)$ transition probabilities in terms of single-particle units ($B_{\text{sp}} = (7/16\pi) e^2 R^6 = 0.42 A^2 e^2 \text{ fm}^6$) are collected. In the last column the oscillator strength (in $B_{\text{sp}} \cdot \text{MeV}$) is displayed. The states listed contribute $\approx 80\%$ of the total energy weighted sum rule. In the last row of this table are listed the properties of the octupole non-collective state used in the calculation of the formfactors of fig. 2. The wavefunctions of three of the states are given in table 4

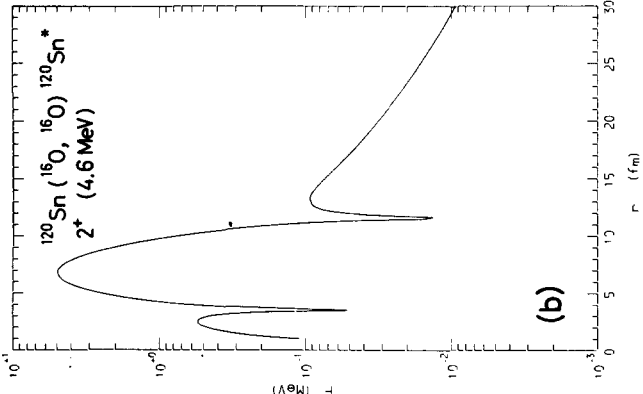
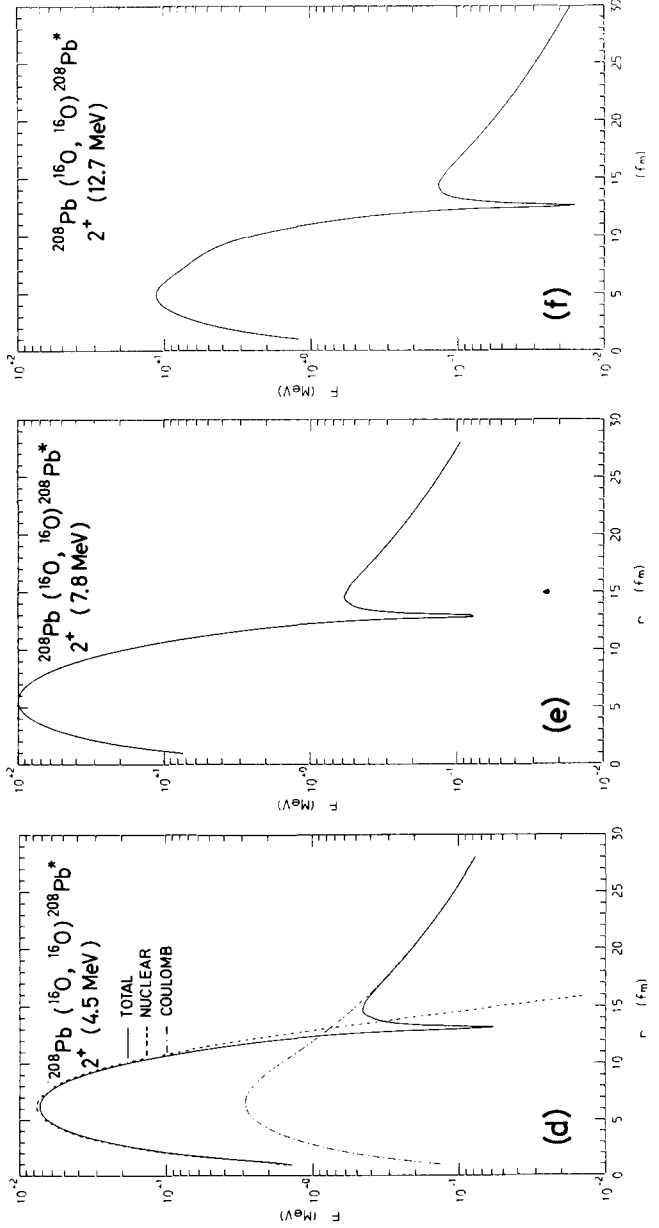
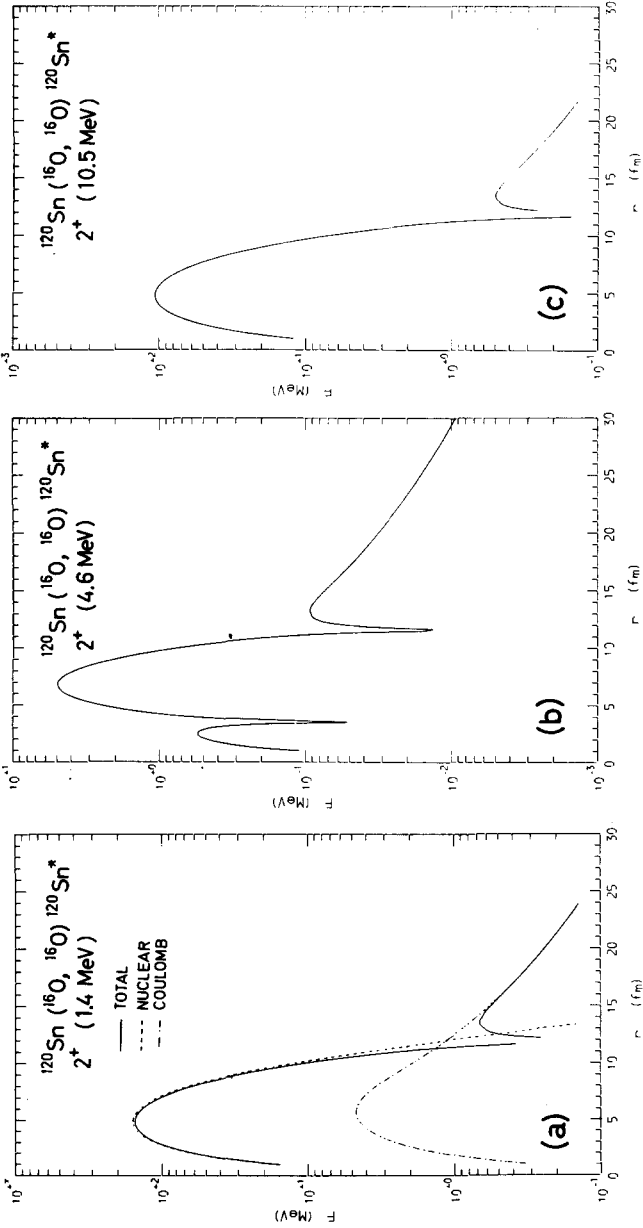
E	E_c	\mathcal{P}	\mathcal{N}	$\Lambda(1/2)/\sqrt{\kappa}$	$\Lambda(-1/2)/\sqrt{\kappa}$	R	RE
2.62	2.62	39.83	57.56	1.48	1.11	20.5	53.71
3.86		21.17	35.78	0.66	0.98	5.40	20.84
5.88	5.04	16.38	34.87	0.32	1.27	3.20	18.82
6.71		13.53	24.77	0.37	0.77	2.2	14.76
							54.42
10.80		13.00	16.00	0.55	0.16	2.03	21.92
13.00	13.50	13.25	9.22	0.74	-0.34	2.10	27.30
14.95		19.41	22.50	0.85	0.13	4.50	67.28
							116.50
27.32		-12.33	19.76	-1.43	2.41	1.80	49.18
29.03	28.81	-11.75	17.79	-1.32	2.22	1.65	47.90
30.11		-12.26	16.65	-1.32	2.19	1.80	54.20
							151.28
6.56	6.56	8.20	11.01	0.09	0.12	0.80	5.28

Utilizing the X and Y amplitudes of ref. [7] and tables 2 and 4 the formfactors for the transitions from the ground state were calculated according to equations (3.8) and (A.4). The single-particle formfactors $f_{\lambda}^{a_1 a_2}(r)$ were calculated using harmonic oscillator wavefunctions. The results are displayed in fig. 2.

For the quadrupole modes in ^{120}Sn and ^{208}Pb the formfactors for the lowest state, a member of the giant isoscalar resonance and a non-collective state are given. A similar selection of states was used for the case of octupole modes in Pb.

At large distances the formfactors display the smooth $r^{-\lambda-1}$ dependence characteristic for Coulomb excitation, the Coulomb excitation formfactor being given separately by a dash-dot curve for the lowest state of each mode. The nuclear part (dashed curve) shows a rapid variation with r . The two contributions have opposite sign and the formfactor thus vanishes at a point close to the sum of the nuclear radii $R_b + R_B$.

Although the magnitude of the different formfactors (in MeV) are quite different their shapes are qualitatively independent of multipolarity and of excitation energy. To emphasize this similarity we compare in fig. 3 some of the results shown in fig. 2. Quasielastic heavy ion reactions are sensitive to the formfactors only in the external region for r -values larger than $R_b + R_B + 2 \text{ fm}$, where all the nuclear formfactors shown are in fact almost identical except for the scale.



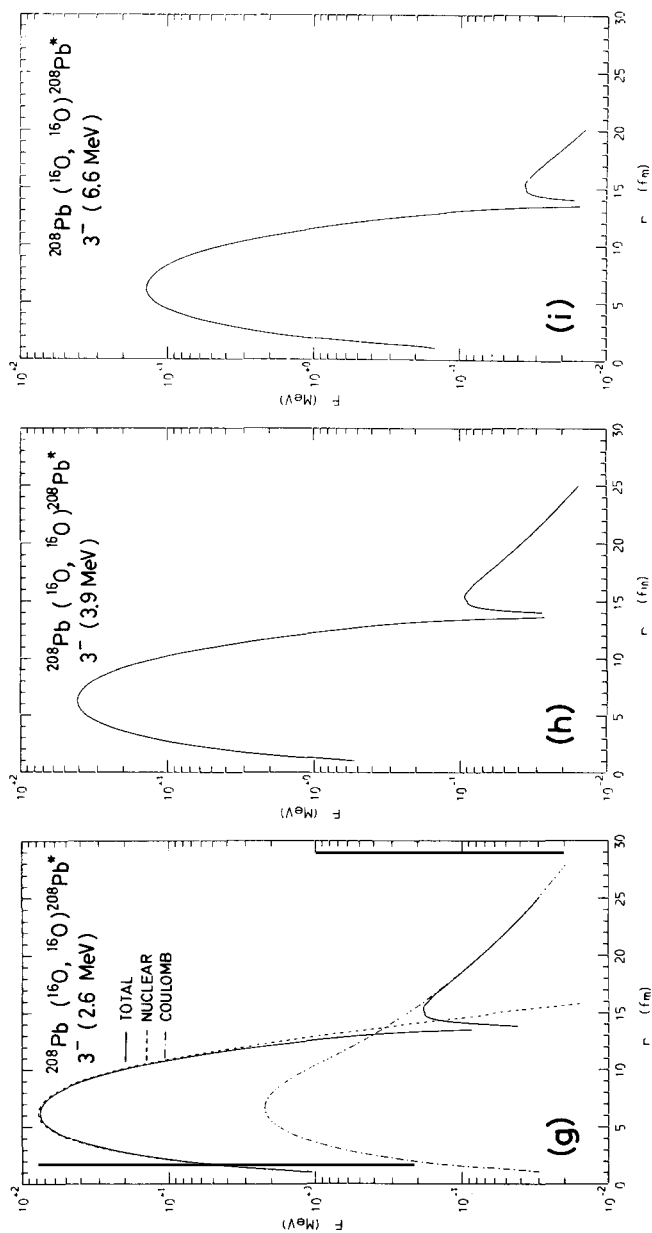


Fig. 2. Microscopic formfactors associated with the inelastic scattering of particle-hole quadrupole vibrations of ^{120}Sn and ^{208}Pb . The formfactors associated with the lowest mode and with the giant isoscalar resonance carrying the largest percentage of the energy weighted sum rule, are displayed in (a) and (c) for Sn and (d) and (e) for Pb as a function of the relative distance. A typical example of a non-collective excitation formfactor is shown in (b) (note the change of scale) and (f) (for Sn and Pb respectively). The energies and transition probabilities of the different states are collected in ref. [7] and in table 1, while the corresponding wavefunctions are collected in tables 6.5 (Pb) and 6.6 (Sn) of ref. [7] and in table 2. The harmonic oscillator parameters determining the single-particle levels utilized in both the Pb and Sn calculations are collected in tables 6.1 and 6.2 of ref. [7]. In the last table the BCS parameters of ^{120}Sn are also given. In order to generate the radial part of the harmonic oscillator wavefunctions entering in the evaluation of the microscopic formfactors through the formula (2.27) we use for protons $\nu = M\omega/\hbar$ with $\hbar\omega \approx 41 A^{-1/3}$ MeV. For neutrons, we required that the mean square radius be equal to that of the protons ($\langle r^2 \rangle_n = \langle r^2 \rangle_p$). Thus the parameters we used are: $\nu_n = 0.245 \text{ fm}^{-2}$, $\nu_p = 0.200 \text{ fm}^{-2}$ for ^{120}Sn and $\nu_n = 0.197 \text{ fm}^{-2}$, $\nu_p = 0.167 \text{ fm}^{-2}$ for ^{208}Pb . In (g), (h) and (i) the microscopic formfactors associated with the inelastic scattering of particle-hole octupole vibrations of ^{208}Pb are given. The wavefunctions utilized in calculating the different formfactors are collected in table 4, while in table 3 we display the value of different matrix elements which characterize the states in question.

Table 4
Wave function associated with three of the octupole states in ^{208}Pb shown in table 3. For details see caption of table 2

N1	L1	J1	N2	L2	J2	2T	DN	E = 2.62		E = 3.86		E = 6.56	
								X	Y	X	Y	X	Y
0.0	6.0	6.5	0.0	5.0	5.5	-1	1	0.88	-0.06	-0.34	-0.04	-0.01	-0.01
1.0	4.0	4.5	1.0	3.0	2.5	+1	1	0.15	-0.02	-0.29	-0.01	-0.01	-0.00
0.0	5.0	4.5	1.0	2.0	1.5	-1	1	-0.15	0.03	-0.65	0.03	0.02	0.00
1.0	4.0	4.5	2.0	1.0	1.5	+1	1	0.27	-0.06	0.51	-0.02	-0.04	-0.01
1.0	3.0	3.5	2.0	0.0	0.5	-1	1	-0.10	0.03	-0.20	0.02	0.02	0.00
0.0	6.0	5.5	1.0	3.0	2.5	+1	1	0.18	-0.06	0.17	-0.02	-0.06	-0.01
1.0	4.0	4.5	0.0	5.0	4.5	+1	1	0.03	-0.01	0.02	-0.00	-0.03	-0.00
2.0	2.0	2.5	2.0	1.0	0.5	+1	1	0.08	-0.03	0.06	-0.01	-0.12	-0.00
0.0	7.0	7.5	0.0	6.0	6.5	+1	1	-0.17	0.07	-0.12	0.03	0.25	0.01
0.0	5.0	4.5	1.0	2.0	2.5	-1	1	0.02	-0.01	0.03	-0.01	0.87	-0.00
2.0	2.0	2.5	1.0	3.0	2.5	+1	1	0.04	-0.02	0.03	-0.01	0.14	-0.00
1.0	4.0	4.5	1.0	3.0	3.5	+1	1	0.09	-0.04	0.05	-0.02	0.24	-0.01
1.0	4.0	3.5	2.0	1.0	0.5	+1	1	0.08	-0.04	0.05	-0.01	0.21	-0.01
0.0	6.0	5.5	0.0	5.0	4.5	+1	1	0.09	-0.04	0.05	-0.02	0.15	-0.01
0.0	5.0	4.5	0.0	4.0	3.5	-1	1	-0.05	0.02	-0.06	0.02	-0.05	0.00
2.0	2.0	2.5	2.0	1.0	1.5	+1	1	0.05	-0.02	0.03	-0.01	0.06	-0.00
1.0	4.0	3.5	1.0	3.0	2.5	+1	1	0.06	-0.03	0.04	-0.01	0.06	-0.00
1.0	3.0	2.5	2.0	0.0	0.5	-1	1	0.03	-0.02	0.04	-0.01	0.02	-0.00
3.0	0.0	0.5	1.0	3.0	2.5	+1	1	0.04	-0.02	0.02	-0.01	0.02	-0.00
2.0	2.0	1.5	1.0	3.0	2.5	+1	1	0.03	-0.02	0.02	-0.01	0.02	-0.00
2.0	2.0	1.5	2.0	1.0	1.5	+1	1	-0.04	0.02	-0.02	0.01	-0.02	0.00
1.0	4.0	3.5	0.0	5.0	4.5	+1	1	0.03	-0.02	0.02	-0.01	0.02	-0.00
2.0	2.0	2.5	1.0	3.0	3.5	+1	1	0.04	-0.02	0.02	-0.01	0.02	-0.00
1.0	4.0	4.5	0.0	5.0	5.5	-1	1	0.03	-0.02	0.03	-0.01	0.01	-0.00
1.0	4.0	4.5	0.0	5.0	5.5	+1	1	0.03	-0.02	0.02	-0.01	0.01	-0.00
0.0	8.0	8.5	0.0	5.0	5.5	-1	3	-0.06	0.04	-0.06	0.03	-0.02	0.00
2.0	2.0	1.5	0.0	5.0	4.5	+1	1	0.02	-0.01	0.01	-0.01	0.01	-0.00
1.0	5.0	5.5	0.0	6.0	6.5	+1	1	-0.04	0.02	-0.02	0.01	-0.02	0.00
3.0	0.0	0.5	1.0	3.0	3.5	+1	1	0.03	-0.02	0.01	-0.01	0.01	-0.00
2.0	2.0	2.5	0.0	5.0	5.5	+1	1	0.02	-0.01	0.01	-0.01	0.01	-0.00
0.0	7.0	7.5	0.0	4.0	4.5	-1	3	0.03	-0.02	0.03	-0.02	0.01	-0.00
0.0	9.0	9.5	0.0	6.0	6.5	+1	3	0.06	-0.04	0.03	-0.02	0.02	-0.01
0.0	8.0	8.5	0.0	5.0	5.5	+1	3	-0.04	0.03	-0.02	0.01	-0.01	0.01
0.0	7.0	6.5	0.0	4.0	3.5	-1	3	0.02	-0.02	0.02	-0.01	0.00	-0.00
0.0	7.0	7.5	0.0	4.0	4.5	+1	3	0.03	-0.02	0.02	-0.01	0.01	-0.00
0.0	8.0	7.5	0.0	5.0	4.5	+1	3	-0.03	0.03	-0.02	0.01	-0.01	0.00
0.0	7.0	6.5	0.0	4.0	3.5	+1	3	0.02	-0.02	0.01	-0.01	0.01	-0.00

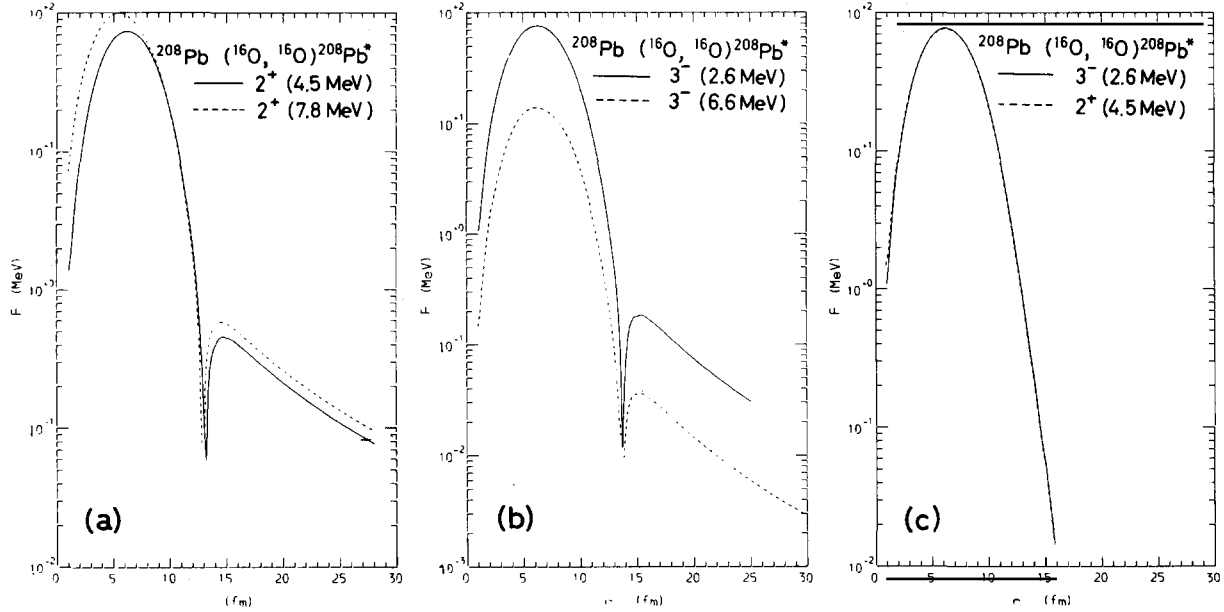


Fig. 3. Comparison between the different microscopic formfactors. In (a) the formfactor for the low-lying 2^+ state of ^{208}Pb is compared to the formfactor associated with the quadrupole giant resonance (cf. fig. 2(d) and (e)). In (b) a collective and a non-collective formfactor for octupole vibrations are compared (cf. fig. 2(g) and 2(i)). In (c) we show the striking similarity of the nuclear part of the formfactor for a quadrupole and an octupole state of ^{208}Pb (cf. fig. 2(d) and 2(g)).

4. Macroscopic formfactors

The strongly collective states of spherical nuclei can be interpreted as vibrational states corresponding to excitations of surface modes. In this macroscopic description the nuclear radius depends on the direction through the expression

$$R_i(r) = R_i^{(0)} \left(1 + \sum_{\lambda\mu} \alpha_{\lambda\mu}(i) Y_{\lambda-\mu}(\vartheta, \varphi) (-1)^\mu \right). \quad (4.1)$$

The quantity $R_i^{(0)}$ is the average radius of the nucleus i while $\alpha_{\lambda\mu}(i)$ indicates the amplitude of the vibrational mode of multipolarity λ .

The Hamiltonian associated with these degrees of freedom is assumed to be [3]

$$H = \sum_{\lambda\mu} \left\{ \frac{1}{2} D_\lambda |\dot{\alpha}_{\lambda\mu}|^2 + \frac{1}{2} C_\lambda |\alpha_{\lambda\mu}|^2 \right\} = \sum_{\lambda\mu} \left\{ \frac{1}{2 D_\lambda} |\pi_{\lambda\mu}|^2 + \frac{1}{2} C_\lambda |\alpha_{\lambda\mu}|^2 \right\}, \quad (4.2)$$

where $\pi_{\lambda\mu}$ is the momentum conjugate to $\alpha_{\lambda\mu}$. The quantities D_λ and C_λ are the mass parameter and the restoring force parameter, respectively. In terms of the boson creation and annihilation operators $c_{\lambda\mu}^+$ and $c_{\lambda\mu}$ the deformation parameters can be written as [3]

$$\alpha_{\lambda\mu} = \sqrt{\frac{\hbar\omega_\lambda}{2C_\lambda}} (c_{\lambda\mu}^+ + (-1)^\mu c_{\lambda-\mu}), \quad (4.3)$$

where ω_λ is the frequency of the mode $\omega_\lambda = \sqrt{C_\lambda/D_\lambda}$.

The parameters entering in the definition of the collective variable (4.3) are determined from the energy of the physical state and from the electromagnetic transition probability which determines the matrix element of the multipole operator $\mathcal{M}(E\lambda, \mu)$. This operator is related to the deformation amplitude by

$$\mathcal{M}_i(E\lambda, \mu) = \frac{3Z_i e(R_i^C)^\lambda}{4\pi} \alpha_{\lambda\mu}(i), \quad (4.4)$$

where R_i^C is the Coulomb radius of nucleus i

$$R_i^C \approx 1.2 A_i^{1/3} \text{ fm}, \quad (4.5)$$

A_i and Z_i being the mass and charge numbers.

In the macroscopic description the detailed interaction V_{bB} between the nuclei b and B is

$$V_{bB} = V_{bB}^N + V_{bB}^C, \quad (4.6)$$

where V_{bB}^C indicates the Coulomb interaction. The nuclear interaction V_{bB}^N is assumed to be a function of the shortest distance between the nuclear surfaces. Neglecting terms quadratic in $\alpha_{\lambda\mu}$ this distance is given by

$$s = r - R_b(-\hat{r}) - R_B(\hat{r}), \quad (4.7)$$

where R_b and R_B are given by (4.1). Terms of similar order of magnitude ($O(\hbar\omega_\lambda/2C_\lambda)$) may arise from a possible dependence of V^N on the radii of curvature. For spherical nuclei discussed below it is however a rather accurate approximation. The case of deformed nuclei, where the equilibrium deformation is of order 0.3, will be discussed in the appendix.

In the following we consider only target excitation and drop the index $i = B$. The formfactor associated with the excitation of the state $|1_{\lambda\mu}\rangle$ with one quantum in the mode $\lambda\mu$ is then given by

$$f(r) = \langle 1_{\lambda\mu} | V_{bB} | 0 \rangle = f^N(r) + f^C(r), \quad (4.8)$$

where $|0\rangle$ indicates the ground state.

The formfactor corresponding to the Coulomb part of (4.6) can be written (cf. also (3.13))

$$f^C(r) = \sum_{\lambda\mu} \frac{4\pi Ze}{(2\lambda + 1)^{3/2}} \langle \lambda || \mathcal{M}_B(E\lambda) || 0 \rangle (-1)^\mu \frac{Y_{\lambda-\mu}(\hat{r})}{r^{\lambda+1}}. \quad (4.9)$$

The nuclear part $f^N(r)$ of the formfactor can be related to the nuclear part of the ion-ion potential $U_{bB}(r)$. This is defined as

$$U_{bB}^N(r) = \langle 0 | V_{bB}^N | 0 \rangle. \quad (4.10)$$

We evaluate now $f^N(r)$ in terms of $U_{bB}^N(r)$. From (4.3) and the corresponding definition for the conjugate operator

$$\pi_{\lambda\mu} = -i\hbar \frac{\partial}{\partial \alpha_{\lambda\mu}} = -i\hbar \sqrt{\frac{C_\lambda}{2\hbar\omega_\lambda}} (c_{\lambda\mu} - (-1)^\mu c_{\lambda-\mu}^+) \quad (4.11)$$

we can express the phonon creation and annihilation operators in terms of $\alpha_{\lambda\mu}$ and $\pi_{\lambda\mu}$, e.g.

$$c_{\lambda\mu} = \sqrt{\frac{C_\lambda}{2\hbar\omega_\lambda}} (-1)^\mu \alpha_{\lambda-\mu} + \sqrt{\frac{\hbar\omega_\lambda}{2C_\lambda}} \frac{\partial}{\partial\alpha_{\lambda\mu}}. \quad (4.12)$$

The formfactor (4.8) is given by

$$f(\mathbf{r}) = \langle 1_{\lambda\mu} | V_{\text{bB}}^{\text{N}}(s) | 0 \rangle = \langle 0 | [c_{\lambda\mu}(\text{B}), V_{\text{bB}}^{\text{N}}] | 0 \rangle = \sqrt{\frac{\hbar\omega_\lambda}{2C_\lambda}} \left\langle 0 \left| \frac{\partial V_{\text{bB}}^{\text{N}}(s)}{\partial\alpha_{\lambda\mu}(\text{B})} \right| 0 \right\rangle. \quad (4.13)$$

Utilizing the relations

$$\frac{\partial V_{\text{bB}}^{\text{N}}(s)}{\partial\alpha_{\lambda\mu}} = -R_{\text{B}}^{(0)} Y_{\lambda\mu}^*(\hat{r}) \frac{\partial V_{\text{bB}}^{\text{N}}(s)}{\partial r} \quad (4.14)$$

and

$$\langle 1_{\lambda\mu} | \alpha_{\lambda\mu} | 0 \rangle = \sqrt{\hbar\omega_\lambda/2C_\lambda}, \quad (4.15)$$

we obtain the result

$$f(\mathbf{r}) = -\sqrt{\frac{\hbar\omega_\lambda}{2C_\lambda}} R_{\text{B}}^{(0)} Y_{\lambda\mu}^*(\hat{r}) \left\langle 0 \left| \frac{\partial V_{\text{bB}}^{\text{N}}}{\partial r} \right| 0 \right\rangle = -\langle 1_{\lambda\mu} | \alpha_{\lambda\mu} | 0 \rangle R_{\text{B}}^{(0)} Y_{\lambda\mu}^*(\hat{r}) \frac{\partial U_{\text{bB}}^{\text{N}}}{\partial r}. \quad (4.16)$$

This expression, which has been widely used for the description of inelastic scattering, has been considered as the lowest order term in an expansion in

$$q = \langle 1_{\lambda\mu} | \alpha_{\lambda\mu} | 0 \rangle R_{\text{A}}^{(0)} d(\log U_{\text{bB}}^{\text{N}})/dr, \quad (4.17)$$

i.e. in the ratio of (4.16) to (4.10). As it is seen from the above derivation this is not the case, the result (4.16) being an exact expression for harmonic vibrations and for the nuclear interaction (4.6)–(4.7). In other words (4.16) represents the first term, not in an expansion in q , but in $\langle 1 | \alpha | 0 \rangle$. This result is essential for the validity of the macroscopic treatment of inelastic scattering since the parameter q is often of the order of unity.

The general matrix element between two many-phonon states is worked out in appendix B.

We have calculated the macroscopic formfactors as discussed above for some of the reactions studied in fig. 2 and the results are given in fig. 4 together with the corresponding microscopic formfactors. In all cases the ion–ion potential $U^{\text{N}}(r)$ was chosen to be the one determined from the experimental analysis of the elastic scattering [9]. In the region of interest it agrees quite well with the one of ref. [8]. The parameters of the Saxon–Woods potentials are given in the fig. 5 caption.

As it is seen from the figure the macroscopic and microscopic formfactors agree well, outside the distance $R_{\text{b}} + R_{\text{B}} + 2$ fm, inside which no contribution to inelastic scattering is expected (cf. also section 6).

The radial part of the formfactors (3.8) and (4.16) are real numbers and are the quantities to be used in a coupled channel treatment of heavy ion reactions. In actual calculations, as e.g. DWBA one takes into account in an empirical way the channels not treated explicitly by introducing an imaginary potential. In elastic scattering the imaginary potential W essentially describes the depopulation of the entrance channel. For inelastic scattering the excited state can be populated via the neglected channels which effectively implies an imaginary contribution to the formfactor. Since the coupling to the neglected channels (i.e. the formfactors) are correlated with the position of the nuclear surface, one would in the macroscopic model expect that the imaginary part of the form-

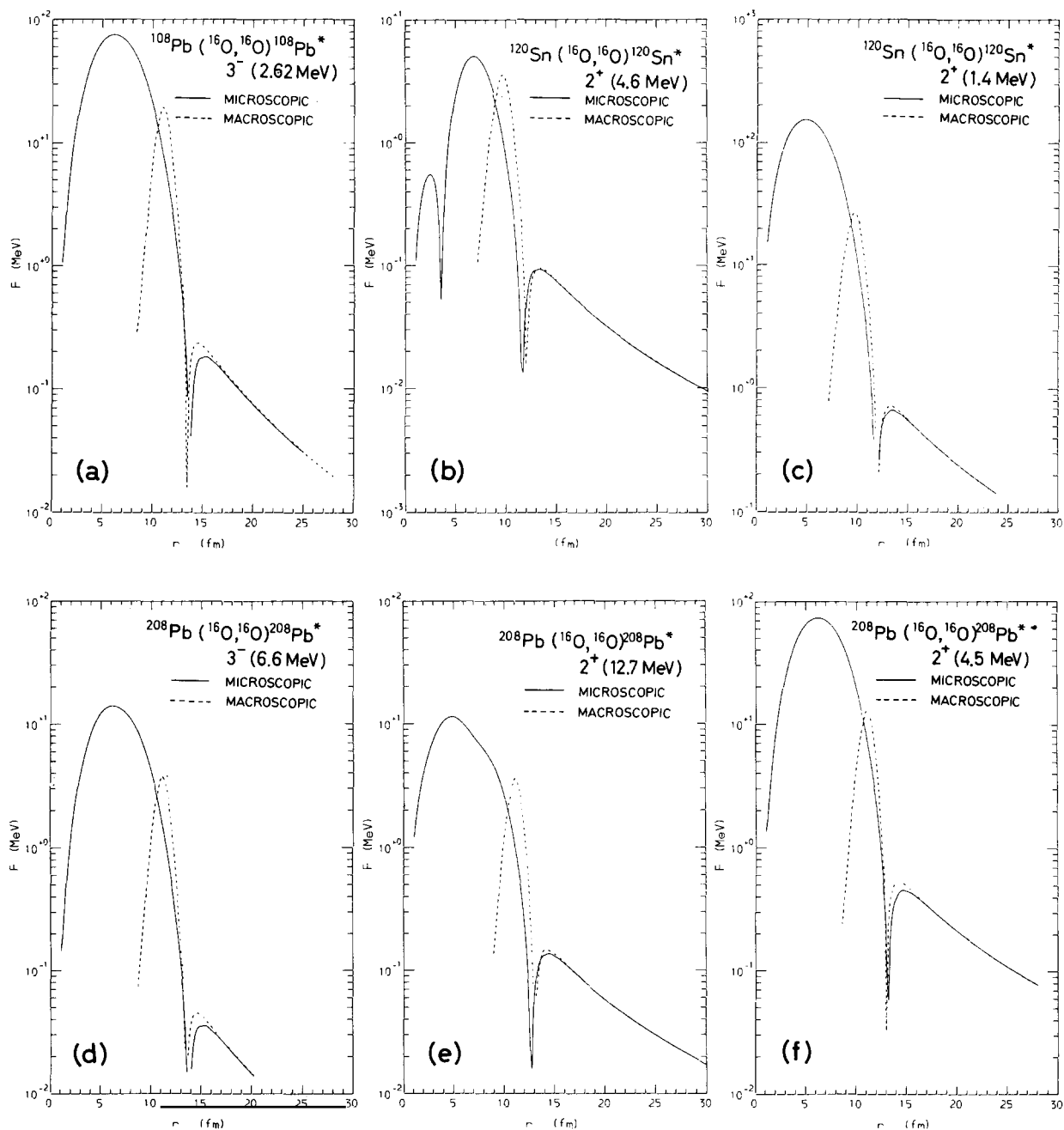


Fig. 4. Macroscopic formfactors for some of the reactions studied in fig. 2. They were calculated using equation (4.22) and the potential determined from elastic scattering in references [9] and [10], adjusting the matrix element of $\alpha_{\lambda\mu}$ to agree with the microscopic result for the matrix element of the multipole operator $\mathcal{M}(E\lambda, \mu)$, which also agrees with the known experimental values. For comparison we display also the corresponding microscopic formfactors taken from fig. 2. Similar good agreements between the two types of formfactors are found using the empirical potential of ref. [8].

factor is correlated to the imaginary part of the elastic potential W in the same way as the real part of the formfactor is correlated to U^N .

This is the standard prescription which will be used also in the applications presented in section 6.

The formfactors for strongly deformed nuclei, where the first order expansion in the deformation parameter is not appropriate, are evaluated in appendix C.

5. Equivalence of macroscopic and microscopic formfactors for collective states

The numerical agreement between the macroscopic and microscopic formfactors shown in the previous section is a natural consequence of the basic assumptions utilized in the RPA. In fact the collective states are generated by the coupling between the particle degrees of freedom and the mean field which in turn is produced by the particles themselves. The collective response of the nucleus to an external field should therefore be the same whether one describes the system in terms of the particle degrees of freedom or in terms of the collective degrees of freedom of the mean field or the associated density.

In order to show this equivalence explicitly we use the expression (2.29) for the formfactor operator. The diagonal matrix element of this operator is identical to the ion-ion potential as calculated by folding, i.e.,

$$U_{bB}(r) = \langle 0 | \hat{f}(r) | 0 \rangle = \int d^3 r'_1 U_{1b}(r'_{1b}) \langle 0 | \hat{\rho} | 0 \rangle, \quad (5.1)$$

while the non-diagonal matrix element is given by

$$\langle \lambda \mu | \hat{f} | 00 \rangle = \int d^3 r_1 U_{1b} \langle \lambda \mu | \hat{\rho} | 0 \rangle. \quad (5.2)$$

We want to consider only the excitation of particle-hole bosons i.e., excitations generated by the boson representation $(\hat{f}(r))_B$ of the formfactor (cf. eq. (3.7)). The matrix elements of the corresponding density-operator $(\hat{\rho})_B$ defined by

$$(\hat{f}(r))_B = \int U_{1b}(r'_{1b}) (\hat{\rho}(r'_{1c}))_B d^3 r'_1, \quad (5.3)$$

can be written in terms of the amplitudes X and Y as

$$\begin{aligned} \langle n, \lambda \mu | (\hat{\rho})_B | 00 \rangle &= \sum_{\substack{a_k a_i \\ m_k m_i}} \int d\xi_1 \phi_{j_i m_i}^* (a_i r_{1c} \xi_1) \phi_{j_k m_k} (a_k r_{1c} \xi_1) [X_n(a_k a_i \lambda) - Y_n(a_k a_i \lambda)] \\ &\times (-1)^{j_k + m_k + \pi_k} \langle j_i - m_i j_k m_k | \lambda - \mu \rangle. \end{aligned} \quad (5.4)$$

The index a_k indicate states above the Fermi surface while a_i designates occupied states.

In the random phase approximation these amplitudes are given by

$$\left. \begin{aligned} X_n(a_k a_i \lambda) \\ Y_n(a_k a_i \lambda) \end{aligned} \right\} = \pm (-1)^{\pi_i} \Lambda_\lambda^n \langle a_k || F_\lambda || a_i \rangle / (\epsilon_{a_k} - \epsilon_{a_i} \mp \hbar \omega_\lambda^n). \quad (5.5)$$

They were obtained by diagonalizing the separable interaction [3]

$$H = \kappa \sum_\mu F_{\lambda\mu} F_{\lambda\mu}^\dagger, \quad (5.6)$$

where

$$\kappa F_{\lambda\mu} = \frac{\partial U_{1C}}{\partial \alpha_{\lambda\mu}^*} \quad (5.7)$$

is the single-particle field generated by the vibration. The quantity Λ_λ^n , indicating the particle-vibration coupling strength

$$\frac{\Lambda_\lambda(n)}{\kappa} = \left\{ \sum_{\substack{a_k a_i \\ m_k m_i}} \frac{4\hbar\omega_\lambda(n)(\epsilon_{a_k} - \epsilon_{a_i}) |\langle a_k m_k | \kappa F_{\lambda\mu} | a_i m_i \rangle|^2}{[(\epsilon_{a_k} - \epsilon_{a_i})^2 - (\hbar\omega_\lambda(n))^2]^2} \right\}^{-1/2}. \quad (5.8)$$

In the actual calculations, the results of which were presented in section 3, one used instead of (5.7) the field $r^\lambda Y_{\lambda\mu}(r)$, which has similar matrix elements as (5.7) except for a common factor.

One may write the matrix element of (5.7) appearing in (5.5) in the form

$$\langle a_k m_k | \kappa F_{\lambda\mu} | a_i m_i \rangle = \left\langle a_k m_k \left[\left[\frac{\partial}{\partial \alpha_{\lambda\mu}^*}, H_{sp} \right] \right] a_i m_i \right\rangle = (\epsilon_{a_k} - \epsilon_{a_i}) \left\langle a_k m_k \left[\frac{\partial}{\partial \alpha_{\lambda\mu}^*} \right] a_i m_i \right\rangle, \quad (5.9)$$

where H_{sp} is the single-particle Hamiltonian being also a function of the deformation parameters $\alpha_{\lambda\mu}$. The matrix elements (5.9) enter in the cranking expression for the mass parameter D_λ in (4.2) i.e.,

$$D_\lambda^n = 2\hbar^2 \sum_{\substack{a_k a_i \\ m_i m_k}} \frac{|\langle a_k m_k | \kappa F_{\lambda\mu} | a_i m_i \rangle|^2}{(\epsilon_{a_k} - \epsilon_{a_i})^3}. \quad (5.10)$$

There are two limits in which we can prove the equivalence between the macroscopic and microscopic formfactors, utilizing the above expressions. In the first limit we assume $\hbar\omega_\lambda \ll (\epsilon_{a_k} - \epsilon_{a_i})$, i.e., the vibrational energy is much smaller than the particle-hole excitation energy. In the second limit we assume that all particle excitations contributing to a given mode are degenerate i.e.,

$$\epsilon_{a_k} - \epsilon_{a_i} = \Delta\epsilon.$$

In both these situations one finds, utilizing the equations (5.5)–(5.10), that the matrix element (5.4) reduces to

$$\begin{aligned} \langle n, \lambda\mu | (\hat{\rho})_B | 00 \rangle &= \sqrt{\frac{\hbar\omega_\lambda}{2C_\lambda}} \sum_{\substack{a_k a_i \\ m_k m_i}} \int d\xi_1 \left[\phi_{i_i m_i}^*(a_i r_{1C} \xi_1) \phi_{j_k m_k}(a_k r_{1C} \xi_1) \left\langle a_k m_k \left[\frac{\partial}{\partial \alpha_{\lambda\mu}} \right] a_i m_i \right\rangle \right. \\ &\quad \left. + \phi_{j_k m_k}^*(a_k r_{1C} \xi_1) \phi_{i_i m_i}(a_i r_{1C} \xi_1) \left\langle a_k m_k \left[\frac{\partial}{\partial \alpha_{\lambda\mu}} \right] a_i m_i \right\rangle^* \right] \\ &= \frac{\partial}{\partial \alpha_{\lambda\mu}} (\langle 0 | \hat{\rho} | 0 \rangle) \langle n \lambda\mu | \alpha_{\lambda\mu} | 00 \rangle. \end{aligned} \quad (5.11)$$

The formfactor (5.2) is thus given by

$$\langle \Lambda\mu | f | 00 \rangle = \frac{\partial}{\partial \alpha_{\lambda\mu}} (\langle 0 | f | 0 \rangle) \langle n \lambda\mu | \alpha_{\lambda\mu} | 00 \rangle = \frac{\partial}{\partial \alpha_{\lambda\mu}} (U_{bB}(r)) \langle n \lambda\mu | \alpha_{\lambda\mu} | 00 \rangle, \quad (5.12)$$

which is identical to (4.16).

Although the two assumptions leading to this identity are not strictly fulfilled for the actual calculations in section 3, the first assumption is the one relevant for the low-lying collective state, while the second is more appropriate for the giant resonances.

The remaining difference between the calculated macroscopic and microscopic formfactors for $r > R_b + R_B + 2$ fm, as seen from fig. 4, is however not expected to be related to the marginal fulfilment of the above approximation. In fact the microscopic formfactors were calculated utilizing harmonic oscillator wavefunctions which do not display the correct asymptotic behaviour. Also the empirical determination of the ion–ion potential leaves some uncertainty as to the exponential slope of this potential. The above contention is supported by the fact that the microscopic formfactors associated with different multi-polarities (cf. fig.3(c)) are essentially identical.

It is an interesting observation that the formfactor for a collective state is not dominated by a few particle–hole configurations, although the single particle formfactor corresponding to “hot orbitals” of low angular momenta is much larger outside the nucleus than the single particle formfactors involving orbitals of high angular momenta. This is because the amplitudes (X and Y) of these configurations are generally larger than those of the former, the matrix elements of $\partial U/\partial r$ being especially large between states of high angular momenta.

6. Differential cross-sections

In this section we show examples in which the formfactors are used to calculate differential cross-sections for inelastic scattering.

The results for 104 MeV ^{16}O ions scattered on ^{208}Pb leading to the 2.62 MeV octupole vibration is shown in fig. 5 utilizing the microscopic formfactor of fig. 2 and the macroscopic formfactor of fig. 4. The angular distributions are very similar as expected from the similarity of the two formfactors at distances larger than $R_b + R_B + 2$ fm (cf. fig. 4(a)).

The angular distributions do not agree however with the experimental data [9]. Utilizing the macroscopic formfactor including the contribution from the empirical imaginary part one obtains a quantitative agreement as shown in fig. 5(b).

7. Conclusions

The rather detailed investigation carried out in this paper on the calculation of the microscopic formfactors show that the macroscopic prescription in most cases is very accurate. This is not only true for low-lying vibrational states as has been checked empirically, but it is also true for the excitation of giant resonances and not-so-collective states. We have shown that this result is to be expected in the random phase approximation for strongly collective states.

We have also shown that macroscopic formfactors for the excitation of vibrational states are more accurate than hitherto assumed being an expansion in the small parameter $\alpha_{\lambda\mu}$ (vibrational amplitude) and not in the apparent expansion parameter $\alpha_{\lambda\mu}R^{(0)}/a$, a is the diffuseness of the ion–ion potential.

We want to acknowledge the help of P.F. Bortignon in the calculation of the microscopic wavefunctions and H. Esbensen and S. Kahana for valuable discussions.

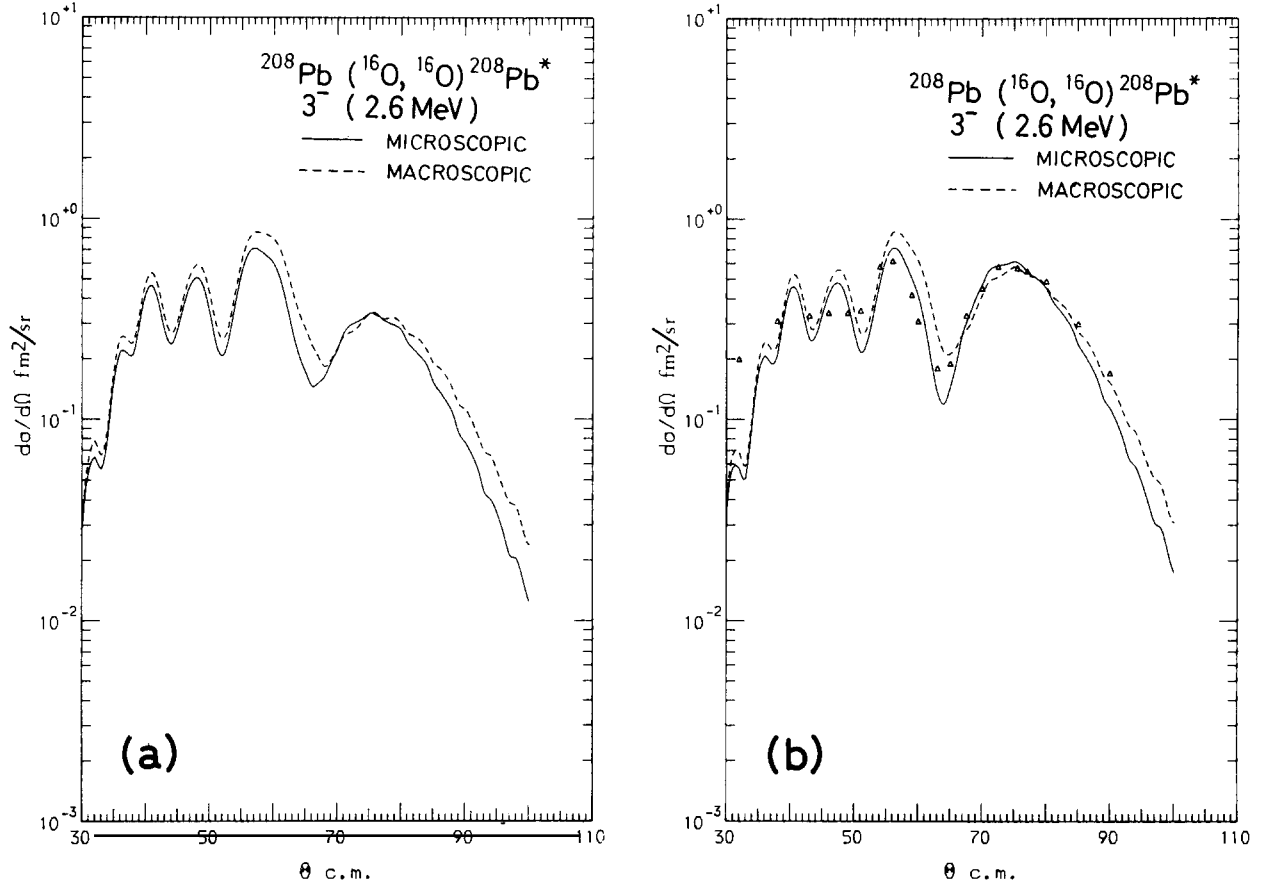


Fig. 5. Theoretical and experimental differential cross-section associated with the excitation of the 2.62 MeV 3^- state in ^{208}Pb with 104 MeV ^{16}O ions. The calculations were carried out in the DWBA utilizing a Saxon-Woods potential with parameters

$$\begin{array}{lll} V = -40 \text{ MeV} & r_v = 1.31 \text{ fm} & a_v = 0.45 \text{ fm} \\ W = -15 \text{ MeV} & r_w = 1.31 \text{ fm} & a_w = 0.45 \text{ fm}. \end{array}$$

In (a) the dashed curve shows the result using the real part of the macroscopic formfactor while the full drawn curve shows the result using the microscopic formfactor of fig. 2(g). In (b) the imaginary part of the macroscopic formfactor was added to both formfactors. The dots indicate the experimental results of ref. [9].

Appendix A: Microscopic formfactors for superfluid and deformed nuclei

In this appendix we calculate inelastic scattering of nuclei showing pairing (superfluid) and surface deformation. For superfluid systems the nuclear states are described in the quasiparticle basis.

The quasiparticle creation and annihilation operators α_{jm}^+ and α_{jm} are defined by the unitary transformation

$$\begin{aligned} a_{j_1 m_1}^+(a_1) &= U_{j_1}(a_1) \alpha_{j_1 m_1}^+(a_1) - (-1)^{j_1 + m_1 + \pi_1} V_{j_1}(a_1) \alpha_{j_1 - m_1}(a_1), \\ b_{j_1 m_1}^+(a_1) &= V_{j_1}(a_1) \alpha_{j_1 m_1}^+(a_1) + (-1)^{j_1 + m_1 + \pi_1} U_{j_1}(a_1) \alpha_{j_1 - m_1}(a_1), \end{aligned} \quad (\text{A.1})$$

where U and V are the BCS occupation parameters. The quasiparticle operators define the vacuum state $|\text{BCS}\rangle$ by the relation

$$\alpha_{jm}(a)|\text{BCS}\rangle = 0. \quad (\text{A.2})$$

In order to evaluate the formfactor for inelastic scattering on superfluid systems one should express (2.23) in terms of these operators. Inserting (A.1) in (2.23) one finds

$$\begin{aligned} \hat{f}(\mathbf{r}) = \sum_{\substack{a_1 a_2 \\ \lambda \mu}} (-1)^{\lambda + \mu + \pi_1} \frac{\sqrt{2j_2 + 1}}{2\lambda + 1} f_{\lambda - \mu}^{a_2 a_1}(\mathbf{r}) \{ U_{j_2}(a_2) V_{j_1}(a_1) [\alpha_{j_2}^+ \alpha_{j_1}^+]_{\lambda \mu} - V_{j_2}(a_2) U_{j_1}(a_1) \\ \times [\beta_{j_2} \beta_{j_1}]_{\lambda \mu} + (U_{j_2}(a_2) U_{j_1}(a_1) - V_{j_2}(a_2) V_{j_1}(a_1)) [\alpha_{j_2}^+ \beta_{j_1}^+]_{\lambda \mu} + (-1)^{\pi_1} V_{j_1}^2(a_1) \sqrt{2j_1 + 1} \\ \times \delta(a_1, a_2) \delta(\lambda, 0) \}, \end{aligned} \quad (\text{A.3})$$

where $\beta_{jm}^+ = (-1)^{j+m+\pi} \alpha_{j-m}$.

The first two terms induce two-quasiparticle excitations, while the third term induces single-quasiparticle excitations and is relevant only for odd nuclei. The last term has only diagonal matrix elements and leads to the ion-ion potential.

In superfluid systems the residual interactions produce collective states which are of similar nature as those discussed in section 3, except that no distinction can be made between particle-hole and two-particle or two-hole states.

Utilizing a relation of the type (3.6) but where $\Gamma_{\lambda\mu}^+(a_1 a_2)$ indicates the two-quasiparticle creation operator and $\Gamma_{\lambda\mu}^+(n)$ indicates the boson creation operator in the quasiparticle basis we obtain for the boson representation of the formfactor an expression identical to (3.7) where the function (3.8) is given by

$$\begin{aligned} f_{\lambda\mu}^n(\mathbf{r}) = \sum_{a_1 > a_2} \frac{(-1)^{\pi_1}}{1 + \delta(a_1, a_2)} \sqrt{\frac{2j_2 + 1}{2\lambda + 1}} f_{\lambda\mu}^{a_2 a_1}(\mathbf{r}) (U_{j_1}(a_1) V_{j_2}(a_2) + U_{j_2}(a_2) V_{j_1}(a_1)) [X_n(a_2 a_1; \lambda) \\ - Y(a_2, a_1; \lambda)]. \end{aligned} \quad (\text{A.4})$$

This expression was used for the numerical evaluation of the formfactor for the excitation of the states in ^{120}Sn displayed in fig. 2.

The macroscopic formfactors for superfluid systems are defined in the same way as for normal systems, as it was done in section 4. The proof of the equivalence of the macroscopic and microscopic formfactors can easily be generalized to include the present case of superfluid systems.

For deformed nuclei the nuclear states are given in terms of the wavefunctions χ_K in the intrinsic frame. We consider only axially symmetric quadrupole deformations where [3]

$$\psi_{I_B M_B} = \sqrt{\frac{2I_B + 1}{16\pi^2(1 + \delta(K_B, 0))}} \{ \mathcal{D}_{M_B K_B}^{I_B}(\vartheta_i) \chi_{K_B}(\xi) + (-1)^{I_B + K_B} \mathcal{D}_{M_B - K_B}^{I_B}(\vartheta_i) \chi_{\bar{K}_B}(\xi) \}. \quad (\text{A.5})$$

The variables ϑ_i denote the three Eulerian angles describing the rotation from the laboratory system to the intrinsic frame, while K_B is the projection of the total angular momentum on the intrinsic z -axis.

In order to evaluate the formfactor connecting states thus described, we express the operator $[a_{j_2}^+(a_2) b_{j_1}^+(a_1)]_{\lambda\mu}$ in (2.23) in terms of the creation operators a'^+ and b'^+ in the intrinsic frame i.e.,

$$[a_{j_2}^+(a_2) b_{j_1}^+(a_1)]_{\lambda\mu} = \sum_{\nu} \mathcal{D}_{\mu\nu}^{\lambda}(\vartheta_i) [a_{j_2}^+(a_2) b_{j_1}^+(a_1)]_{\lambda\nu}. \quad (\text{A.6})$$

Next we express a'^+ and b'^+ in terms of the creation operators of single-particle (Nilsson) states in the deformed average potential. We thus obtain

$$a_{j_2\omega_2}^+(a_2) = \sum_p W_p^{a_2}(\omega_2) a_{\omega_2}^+(p), \quad (\text{A.7})$$

and

$$b_{j_1\omega_1}^+(a_1) = \sum_q W_q^{a_1}(\omega_1) b_{\omega_1}^+(q). \quad (\text{A.8})$$

Utilizing (A.6)–(A.8) we can write the formfactor (2.23) as

$$\hat{f}(\mathbf{r}) = \sum_{\lambda\mu,\nu} \mathcal{D}_{-\mu\nu}^{\lambda}(\vartheta_i) \mathcal{D}_{-\mu 0}^{\lambda*}(\hat{r}) \sum_{\substack{p,q \\ \omega_1 \omega_2}} f_{\lambda\nu}^{pq}(\mathbf{r}) a_{\omega_2}^+(p) b_{\omega_1}^+(q), \quad (\text{A.9})$$

where the intrinsic formfactor is given by

$$f_{\lambda\nu}^{pq}(\mathbf{r}) = \sum_{a_1 a_2} (-1)^{\lambda+\pi_1} \sqrt{\frac{2j_2+1}{4\pi(2\lambda+1)}} \langle j_2\omega_2 j_1\omega_1 | \lambda\nu \rangle W_p^{a_2}(\omega_2) W_q^{a_1}(\omega_1) f_{\lambda}^{a_2 a_1}(\mathbf{r}). \quad (\text{A.10})$$

Note that the summation over μ can be performed leading to a D -function $D_{0\nu}^{\lambda}(\vartheta'_i)$ where ϑ'_i indicates the rotation from the “intrinsic” system with z axis along \mathbf{r} to the intrinsic system of the deformed nucleus.

The residual interaction among the particles moving in the deformed potential gives rise to collective vibrations of particle–hole type. This interaction can also be diagonalized in the RPA and the calculation proceeds in a similar way as for the spherical case discussed in section 3, but for the fact that the quadrupole–quadrupole interaction with $K=1$ should be left out since the vibrational amplitude α_{21} corresponds to a rigid rotation of a quadrupole deformed system which is not allowed in the intrinsic frame. Thus, quadrupole modes are generated by the residual interaction only corresponding to β - and γ -vibrations.

In analogy to (3.1) we define the boson operator

$$\Gamma_{\nu}^+(n) = \sum_{ki} \{X_n(ki) \Gamma_{\nu}^+(ki) + (-1)^{\nu} Y_n(ki) \Gamma_{-\nu}(ki)\}, \quad (\text{A.11})$$

where

$$\Gamma_{\nu}^+(ki) = a_{\omega_k}^+(k) b_{\omega_i}^+(i), \quad (\text{A.12})$$

with $\omega_k + \omega_i = \nu$. The indices k and i label the states above and below the Fermi surface, respectively. The X and Y coefficients are determined by diagonalizing the residual interaction in the RPA. The resulting formfactor obtained by inserting the inverse relation to (A.11) in (A.9) reads

$$\hat{f}(\mathbf{r}) = \sum_{\lambda\mu,\nu} \mathcal{D}_{-\mu\nu}^{\lambda}(\vartheta_i) \mathcal{D}_{-\mu 0}^{\lambda*}(\hat{r}) \sum_n f_{\lambda\nu}^n(\mathbf{r}) \{\Gamma_{\nu}^+(n) + (-1)^{\nu} \Gamma_{-\nu}(n)\}, \quad (\text{A.13})$$

where

$$f_{\lambda\nu}^n(r) = \sum_{ki} \{X_n(ki) - Y_n(ki)\} f_{\lambda\nu}^{ki}(r). \quad (\text{A.14})$$

This formfactor has no diagonal matrix elements. The excitations within the ground state rotational band are generated by the diagonal matrix element in the intrinsic coordinates of the representation (A.9) of the formfactor.

Most deformed nuclei are also superfluid. One has thus to work with intrinsic wavefunction calculated in the quasiparticle representation. The quasiparticle creation and annihilation operators α^+ and α are defined by the two-dimensional rotation in gauge space

$$a'^+_{\omega}(p) = U(p) \alpha^+_{\omega}(p) - V(p) \alpha^-_{\bar{\omega}}(p) \quad (\text{A.15})$$

and

$$b'^+_{\omega}(p) = U(p) \alpha^-_{\bar{\omega}}(p) + V(p) \alpha^+_{\omega}(p). \quad (\text{A.16})$$

The formfactor in the fermion representation takes the form

$$\begin{aligned} \hat{f}(r) = & \sum_{\lambda\mu, \nu} \mathcal{D}^{\lambda}_{-\mu\nu}(\vartheta_i) \mathcal{D}^{\lambda*}_{-\mu 0}(\hat{r}) \sum_{\substack{pq \\ \omega_p \omega_q}} f_{\lambda\nu}^{pq}(r) \{U(p) V(q) \alpha^+_{\omega_p}(p) \alpha^+_{\omega_q}(q) - V(p) U(q) \alpha^-_{\bar{\omega}_p}(p) \alpha^-_{\bar{\omega}_q}(q) \\ & + (U(p) U(q) + V(p) V(q)) \alpha^+_{\omega_p}(p) \alpha^-_{\bar{\omega}_q}(q) - V^2(p) \delta(\bar{p}, q)\}. \end{aligned} \quad (\text{A.17})$$

The last term induces excitations within the ground state band besides being responsible for the ion-ion potential. It is noted that the excitations within the ground state rotational band does not necessarily proceeds through quadrupole transitions although the average intrinsic potential was assumed to be quadrupole deformed.

In order to get the boson representation of the formfactor (A.17) we have to work out the first two terms of this expression in the way outlined in section 3. Thus the operator $\Gamma^+_{\lambda\mu}(a_2 a_1)$ must be replaced by the operator $\Gamma^+_p(\alpha_2 \alpha_1)$ creating a two quasi-particle state out of the deformed vacuum, and the boson operators $\Gamma^+_{\lambda\mu}(n)$ must be replaced by the corresponding operator $\Gamma^+_p(n)$. Apart from the coefficients W of the Nilson expansion, the result is thus similar to the one in (A.4).

Appendix B: Matrix elements between multi-phonon states

In this appendix we calculate the matrix element

$$\langle n_{\lambda\mu} | V^N(s) | m_{\lambda\mu} \rangle = \frac{1}{\sqrt{n_{\lambda\mu}! m_{\lambda\mu}!}} \langle 0 | (c_{\lambda\mu})^{n_{\lambda\mu}} V^N(s) (c^+_{\lambda\mu})^{m_{\lambda\mu}} | 0 \rangle \quad (\text{B.1})$$

of the nuclear interaction V^N between two many-phonon states.

Utilizing the result (4.13) i.e.,

$$[c_{\lambda\mu}, V^N] = \langle 1_{\lambda\mu} | \alpha_{\lambda\mu} | 0 \rangle \partial V^N / \partial \alpha_{\lambda\mu} \quad (\text{B.2})$$

and defining

$$[c_{\lambda\mu}, V^N]^{(n)} = [c_{\lambda\mu}, [c_{\lambda\mu}, V^N]^{(n-1)}], \quad (\text{B.3})$$

we obtain

$$[c_{\lambda\mu}, V^N]^{(n)} = (\langle 1_{\lambda\mu} | \alpha_{\lambda\mu} | 0 \rangle \partial / \partial \alpha_{\lambda\mu})^n V^N. \quad (\text{B.4})$$

Making use of this relation we can calculate the result of commuting all the destruction operators with V^N in eq. (B.1). Assuming $n < m$ we obtain

$$\begin{aligned} \langle 0 | (c_{\lambda\mu})^{n\lambda\mu} V^N (c_{\lambda\mu}^+)^{m\lambda\mu} | 0 \rangle &= \sum_{p=0}^n \binom{n\lambda\mu}{p} \langle 0 | [c_{\lambda\mu}, V^N]^{(n\lambda\mu-p)} (c_{\lambda\mu})^p (c_{\lambda\mu}^+)^{m\lambda\mu} | 0 \rangle \\ &= \sum_{p=0}^n \binom{n\lambda\mu}{p} \left(-\langle 1_{\lambda\mu} | \alpha_{\lambda\mu} | 0 \rangle R_A^{(0)} Y_{\lambda\mu}^* \frac{\partial}{\partial r} \right)^{n\lambda\mu-p} \langle 0 | V^N (c_{\lambda\mu})^p (c_{\lambda\mu}^+)^{m\lambda\mu} | 0 \rangle. \end{aligned} \quad (\text{B.5})$$

Utilizing the boson commutation relation we obtain

$$(c_{\lambda\mu})^p (c_{\lambda\mu}^+)^{m\lambda\mu} | 0 \rangle = \frac{m_{\lambda\mu}!}{(m_{\lambda\mu} - p)!} (c_{\lambda\mu}^+)^{m\lambda\mu - p} | 0 \rangle. \quad (\text{B.6})$$

The matrix element appearing in the summation in (B.5) can thus be written as

$$\langle 0 | V^N (c_{\lambda\mu})^p (c_{\lambda\mu}^+)^{m\lambda\mu} | 0 \rangle = \frac{m_{\lambda\mu}!}{(m_{\lambda\mu} - p)!} \langle 0 | V^N (c_{\lambda\mu}^+)^{m\lambda\mu - p} | 0 \rangle. \quad (\text{B.7})$$

This matrix element can be calculated utilizing (B.4) i.e.

$$\langle 0 | V^N (c_{\lambda\mu}^+)^{m\lambda\mu - p} | 0 \rangle = \langle 0 | (c_{\lambda\mu})^{m\lambda\mu - p} V^N | 0 \rangle^* = \left(-\langle 1_{\lambda\mu} | \alpha_{\lambda\mu} | 0 \rangle R_A^{(0)} Y_{\lambda\mu} \frac{\partial}{\partial r} \right)^{m\lambda\mu - p} \langle 0 | V^N | 0 \rangle. \quad (\text{B.8})$$

The total matrix element (B.5) is thus equal to

$$\begin{aligned} \langle n_{\lambda\mu} | V^N | m_{\lambda\mu} \rangle &= \sum_{p=0}^n \frac{(n_{\lambda\mu}! m_{\lambda\mu}!)^{1/2}}{p! (n_{\lambda\mu} - p)! (m_{\lambda\mu} - p)!} \left(-\langle 1_{\lambda\mu} | \alpha_{\lambda\mu} | 0 \rangle R_A^{(0)} \right)^{m_{\lambda\mu} + n_{\lambda\mu} - 2p} (Y_{\lambda\mu})^{m_{\lambda\mu} - p} \\ &\quad \times (Y_{\lambda\mu}^*)^{n_{\lambda\mu} - p} \left(\frac{\partial}{\partial r} \right)^{m_{\lambda\mu} + n_{\lambda\mu} - 2p} U^N. \end{aligned} \quad (\text{B.9})$$

Appendix C: Macroscopic formfactors for deformed nuclei

For deformed nuclei the macroscopic description of the formfactors is most conveniently worked out utilizing a formulation analogous to (2.29). We thus introduce the ion-ion potential as a function of the deformation parameters of the form

$$U(\mathbf{r}, \alpha_{\lambda\mu}) = \int \rho_B(\mathbf{r}', \alpha_{\lambda\mu}) U_{\text{ib}}(|\mathbf{r}' - \mathbf{r}|) d^3r'. \quad (\text{C.1})$$

In evaluating the integral (C.1) we use a coordinate system in which the z-axis is along the symmetry axis of the equilibrium deformation. We thus assume that

$$\rho_B(\mathbf{r}, \alpha_{\lambda\mu}) = \rho_B \left(r - R_B^{(0)} [1 + (a_{20}^{(0)} + a_{20}) Y_{20}^* + a_{22}(Y_{22} + Y_{2-2}^*) + \sum_{\lambda \geq 3, \nu} a_{\lambda\nu} Y_{\lambda\nu}^*] \right), \quad (\text{C.2})$$

where $a_{20}^{(0)}$ is the equilibrium deformation. The vibrational amplitudes a_{20} and a_{22} give rise to β - and γ -vibrations respectively.

The formfactor for excitations within the ground state rotational band are given by taking matrix elements of (C.1) between wavefunctions of the type (A.5). We shall consider even nuclei and write the wavefunction in the form

$$|I_B \nu M_B\rangle = \sqrt{\frac{2I_B + 1}{8\pi^2}} \mathcal{D}_{M_B \nu}^{I_B}(\vartheta_i) |n, \lambda \nu\rangle \quad (\text{C.3})$$

where $|n\lambda\nu\rangle$ indicates a state with zero ($n = 0$) or one ($n = 1$) quantum of multipolarity λ and K-quantum number ν , i.e. an eigenstate of the vibrations in the variable $a_{\lambda\nu}$.

The formfactor for excitations within the ground state rotational band is given by

$$\langle I_B 0 M_B | U_{bB}(\mathbf{r}, \alpha_{\lambda\mu}) | 000 \rangle = \sqrt{\frac{2I_B + 1}{8\pi^2}} \int d^3 \vartheta_i \mathcal{D}_{M_B 0}^{I_B*}(\vartheta_i) U_{bB}^{\text{int}}(\mathbf{r}, \hat{r} \cdot \hat{3}, \alpha_{20}^{(0)}), \quad (\text{C.4})$$

where the ion-ion potential in the intrinsic frame is defined by

$$U_{bB}^{\text{int}}(\mathbf{r}) = \int d^3 r' \langle 000 | \rho(r') | 000 \rangle U_{\text{ib}}(|r' - r|). \quad (\text{C.5})$$

This quantity is a function of r and the angle between \mathbf{r} and the intrinsic symmetry axis (3).

The expression (C.4) can be calculated making use of the relation

$$\mathcal{D}_{M_B 0}^{I_B}(\vartheta_i) = \sum_{M'} \mathcal{D}_{M_B M'}^{I_B}(\varphi, \theta, \psi) \mathcal{D}_{M' 0}^{I_B}(\vartheta'_i), \quad (\text{C.6})$$

where the three Eulerian angles (φ, θ, ψ) indicate the rotation from the laboratory system to a system with z-axis along \mathbf{r} , while the Eulerian angles ϑ'_i indicate the orientation of the intrinsic system with respect to this coordinate system.

Inserting (C.6) in (C.4), the integration over two of the Eulerian angles can be performed and we find

$$\langle I_B 0 M_B | U_{bB}(\mathbf{r}, \alpha_{\lambda\mu}) | 000 \rangle = f_{I_B}(r) Y_{I_B M_B}^*(\hat{r}), \quad (\text{C.7})$$

with

$$f_{I_B}(r) = \sqrt{\pi} \int \sin \vartheta' d\vartheta' P_{I_B}(\cos \vartheta') U_{bB}^{\text{int}}(r, \vartheta', \alpha_{20}^{(0)}). \quad (\text{C.8})$$

The non-diagonal matrix elements of (C.1) in the intrinsic states can be treated in the same way as the non-diagonal matrix element in section 4, i.e. one may use

$$\langle 1\lambda\nu | \rho | 000 \rangle = -R_B^{(0)} Y_{\lambda\nu}^*(\hat{r}') \langle 1\lambda\nu | a_{\lambda\nu} | 000 \rangle \partial \langle 0 | \rho | 0 \rangle / \partial r', \quad (\text{C.9})$$

which holds to the same degree of accuracy as (4.16).

The formfactor (C.8) can be evaluated analytically if we use an exponential ion-ion potential of the form

$$U_{bB}^N(r) = -S\bar{R} e^{-(r - R_b - R_B)/a}, \quad (\text{C.10})$$

where (cf. ref. [8]) $S \approx 50$ MeV/fm and $a \approx 0.63$ fm. The quantity \bar{R} is given by [11]

$$\bar{R} = (c_{\parallel}^b + c_{\parallel}^B)^{-1/2} (c_{\perp}^b + c_{\perp}^B)^{-1/2}, \quad (\text{C.11})$$

where the c 's are related to the radii of curvature at the point of contact between b and B . We shall assume that b is spherical i.e., R_b is constant and

$$c_{\parallel}^b = c_{\perp}^b = 1/R_b. \quad (\text{C.12})$$

For the radius R_B of nucleus B we assume the angular dependence corresponding to an axially deformed equilibrium shape i.e., in the intrinsic frame

$$R_B = R_B^{(0)}(1 + \epsilon_2 P_2(\cos \vartheta')), \quad (\text{C.13})$$

with

$$\epsilon_2 = \sqrt{5/4\pi} a_{20}^{(0)}. \quad (\text{C.14})$$

The quantities c_{\parallel}^B and c_{\perp}^B are then the principal rates of curvature at the point of contact. We shall use the expression

$$\bar{R}_{bB} = \frac{R_b R_B^{(0)}}{R_b + R_B^{(0)}} (1 - B_2 P_2(\cos \vartheta')). \quad (\text{C.15})$$

with

$$B_2 = \frac{2R_b}{R_b + R_B^{(0)}} \epsilon_2, \quad (\text{C.16})$$

which is correct to first order in B_2 .

Inserting (C.13) and (C.15) in (C.10) we find in the intrinsic frame

$$U_{bB}^{\text{int}}(r, \vartheta') = -S \frac{R_b R_B^{(0)}}{R_b + R_B^{(0)}} (1 - B_2 P_2(\cos \vartheta')) \exp \{-(r - R_b - R_B^{(0)}(1 + \epsilon_2 P_2(\cos \vartheta')))/a\}. \quad (\text{C.17})$$

In evaluating the integral (C.8) it is not appropriate to expand the exponential in (C.17) in powers of β_2 since the expansion parameter

$$c = (R_B^{(0)}/a) \epsilon_2 \quad (\text{C.18})$$

is often of the order of magnitude of unity. The integral can however, be evaluated in terms of the functions given in ref. [5] (page 219) i.e.,

$$q_I(c) = \frac{1}{2} \int_{-1}^1 dx P_I(x) e^{cP_2(x)} = \frac{\Gamma((I+1)/2)}{2\Gamma((2I+3)/2)} e^{c(\frac{3}{2})^{I/2}} {}_1F_1\left(\frac{I+2}{2}, \frac{2I+3}{2}, \frac{-3}{2}c\right), \quad (\text{C.19})$$

where ${}_1F_1$ is a confluent hypergeometric function.

The quantities $q_I(c)$ satisfy the following recursion relation

$$(I+2)(2I-1)q_{I+2}(c) = \left(1 - \frac{(2I-1)(2I+3)}{3c}\right)(2I+1)q_I(c) + (I-1)(2I+3)q_{I-2}(c), \quad (\text{C.20})$$

and they can therefore be evaluated from $q_0(c)$ and $q_{-2}(c)$ which according to (C.19) are given by

$$q_0(c) = e^{-c/2} \sqrt{\frac{\pi}{-6c}} \operatorname{erf} \left(\sqrt{-\frac{3c}{2}} \right),$$

$$q_{-2}(c) = \frac{1}{3c} e^c, \tag{C.21}$$

where $\operatorname{erf}(x)$ is the error function. The functions $q_I(c)$ are given in fig. 6 for $I = 0, 2$ and 4 .

In order to evaluate the integral (C.8) in terms of $q_I(c)$ we note that the term proportional to B_2 can be expressed in terms of dq_I/dc . We may therefore, to first order in B_2 write the result

$$f_I(r) = \sqrt{4\pi} (U_{bB}^N(r))_{\epsilon_2=0} q_I \left(c \left(1 - \frac{2a R_b}{R_B^{(0)}(R_b + R_B^{(0)})} \right) \right) \tag{C.22}$$

where $(U_{bB}^N(r))_{\epsilon_2=0}$ is the ion-ion potential for deformation zero.

The fact that all formfactors (C.22) have the same radial shape is a consequence of the exponential form of the ion-ion potential, which is expected to be a rather good approximation for heavy ion reactions. Comparing with fig. 6 it is seen that the curvature effect, as was to be expected tends to cancel the first term. Corrections to (C.22) are expected to arise from a possible variation of a with angle and from a change in the value of $R_B^{(0)}$ as compared to the value for non-deformed nuclei [8]

$$R_i^{(0)} = 1.233 A_i^{1/3} - 0.978 A_i^{-1/3}. \tag{C.23}$$

One might thus expect a correction due to volume conservation which, for the spheroidal shape used, would lead to a radius parameter

$$R_B'^{(0)} = R_B^{(0)} \left(1 - \frac{1}{5} \epsilon_2^2 \right), \tag{C.24}$$

to lowest order in ϵ_2^2 .

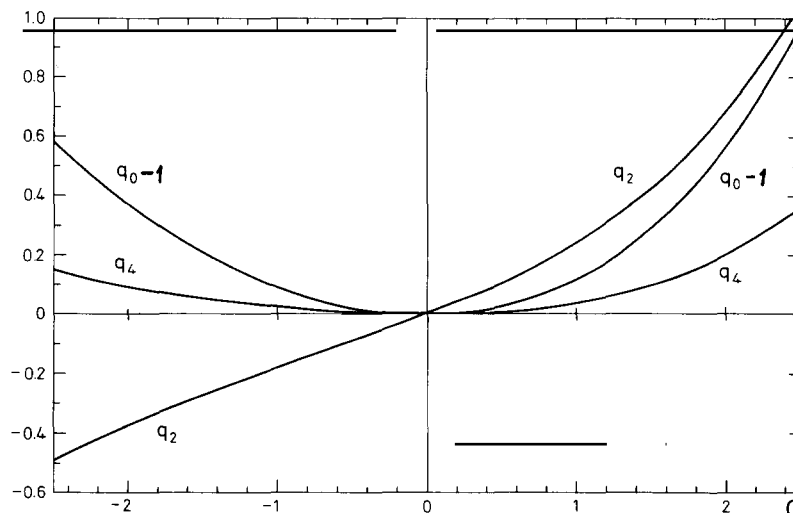


Fig. 6. The functions $q_I(c)$ defined in eq. (C.19). These functions which describe the strength of the ion-ion potential and of the formfactors for excitation within the ground state rotational band (cf. eq. (C.22)) are plotted as functions of the dimensionless parameter c defined in (C.18).

Including this correction the expression (C.22) for the formfactor would read

$$f_I(r) = \sqrt{4\pi} (U_{bB}^N(r))_{\beta_2=0} q_I \left(c \left(1 - \frac{2a R_b}{R_B^{(0)}(R_b + R_B^{(0)})} \right) \right) \left(1 - \frac{a}{5R_B^{(0)}} c^2 \right). \quad (\text{C.25})$$

For many deformed nuclei the ion-ion potential ($U_{bB}^N(r) = (4\pi)^{-1/2} f_0(r)$) according to this formula is almost the same as the potential between the corresponding spherical nuclei. The deformation implies a small increase in the effective range of interaction, but no change in the diffuseness parameter. These conclusions are based on the exponential form of the potential, and are only expected to be correct for

$$r \gtrsim R_b + R_B^{(0)}(1 + |\epsilon_2|) + 1.5 \text{ fm}. \quad (\text{C.26})$$

References

- [1] G.R. Satchler, Nucl. Phys. A279 (1977) 493;
J.B. Ball et al., Nucl. Phys. A252 (1975) 208.
- [2] N. Austern, Direct nuclear reaction theories (Wiley-Interscience, New York, 1970).
- [3] A. Bohr and B.R. Mottelson, Nuclear structure Vol. II (Benjamin, New York, 1975).
- [4] R.A. Broglia, R. Liotta, B.S. Nilsson and A. Winther, Phys. Reports 29C (1977) 291.
- [5] K. Alder and A. Winther, Electromagnetic excitation (North-Holland Publ. Co., Amsterdam, 1975).
- [6] P.F. Bortignon, R.A. Broglia, D. Bes and R. Liotta, Phys. Reports 30C (1977) 305 and references therein.
- [7] D.R. Bes, R.A. Broglia and B.S. Nilsson, Phys. Reports 16C (1975) 1.
- [8] P.R. Christensen and A. Winther, Phys. Lett. 65B (1976) 19.
- [9] F. Becchetti, D.G. Kovar, B.G. Harvey, J. Mahoney, B. Mayer and F.G. Pühlhofer, Phys. Rev. C6 (1972) 2215.
- [10] B.C. Robertson, J.T. Sample, D.R. Goosman, K. Nagatani and K.W. Jones, Phys. Rev. C4 (1971) 2176.
- [11] J. Błocki, J. Randrup, W.J. Swiatecki and C.F. Tsang, Annals of Physics 105 (1977) 427.